TOPSAFE

Dubrovnik, Croatia, 30.09 - 3.10.2008

TopSafe 2008

Transactions

Dubrovnik, Croatia
30.9. - 3.10.2008

HND

AEN NEA

IAEA International Atomic Energy Agency
Atoms For Peace

European Nuclear Society
Rue Belliard 65
1040 Brussels, Belgium
Phone + 32 2 505 30 54
Fax +32 2 502 39 02
E-mail ens@euronuclear.org
Internet www.euronuclear.org

ISBN 978-92-95064-06-5

These transactions contain all contributions submitted by 30 September 2008.

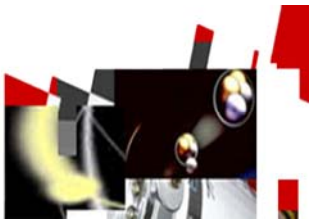

Fuel Cylcle Safety

CRISTAL: A French Criticality Code Package to Assess AREVA NP Nuclear Installation Criticality Safety

M. Doucet, N. Comte, L. Durand Terrasson, Ch. Faignet, M. Landrieu, S. Zheng
AREVA NP – An AREVA and Siemens Company - DSBU
10, rue J. Récamier, 69006 Lyon, France
michel.doucet@areva.com, nadine.comte@areva.com,
laurence.durand-terrasson@areva.com, christine.faignet@areva.com,
michel.landrieu@areva.com, songhui.zheng@areva.com

ABSTRACT

For more than thirty years, CEA (Commissariat à l'Energie Atomique, the French Atomic Energy Agency), IRSN (Institut de Radioprotection et de Sûreté Nucléaire, the Institute for Radioprotection and Nuclear Safety) and the French nuclear industry have been combining their efforts to finance, develop and validate computer codes to assess the criticality safety concerns of nuclear installations, transport casks, and reprocessing facilities. As one of the major world fuel vendors, AREVA NP is deeply involved in defining code developments which incorporate feedback from both users and customers. The result of these continuous efforts is the evolutionary CRISTAL code.

The CRISTAL package was developed as an easy-to-use system using cross-section libraries (JEF 2.2 and CEA93), well-established computer codes (APOLLO2, MORET 4 and TRIPOLI-4) and including a Graphical User-Friendly Interface. The APOLLO2 computer code, a spectral code used for evaluating the basic characteristics of fuel assemblies, has been upgraded to perform criticality safety calculations. The MORET 4 computer code is a neutron simulation code in three dimensions which uses the multigroup formalism for cross-sections and the Monte Carlo method to solve the Boltzmann equation.

Through the years, the CRISTAL package has been improved to take into account both the growth of its validation database and the increasing user requirements. Today, CRISTAL V0 is an up-to-date computational tool incorporating the comprehensive APOLLO2 and MORET 4 computer codes; CRISTAL V0 is the result of more than five years of development work focusing on theoretical approaches and on the implementation of user-friendly graphical interfaces.

Thanks to its broad validation database, CRISTAL V0 provides outstanding accuracy of criticality evaluation for configurations covering the entire fuel cycle life (i.e. from fuel enrichment, pellet/assembly fabrication and transport casks to fuel reprocessing). With more than a thousand benchmark/calculation comparisons, uncertainties can be deduced for various file media, fissile shapes, fissile process interactions, neutron-poisoning screens and material reflectors. These uncertainties, combined with suitable modelling features, ensure confidence in the CRISTAL results when justifying sufficient safety margins.

After a brief description of the calculation scheme and the physics algorithms used in the codes, various industrial applications encountered in a UO2 fuel fabrication plant will be discussed.

1 INTRODUCTION

Criticality safety is a concern for fissile material during all stages of the fuel fabrication process. In this paper, typical processes for a UO2 fuel fabrication plant (including UF6 cylinder storage, UF6-UO2 conversion, powder storage, pelletizing, rod loading, and assembly fabrication) are investigated.

Safety implementation is based on criticality analyses and existing subcriticality margins with consideration of actual safety assessments and process requirements. The accuracy of a criticality calculation produces confidence when addressing safety concerns. The CRISTAL code package [1], with its large qualification database, can provide this high level of confidence.

2 THE CRISTAL CODE PACKAGE

The CRISTAL code package was developed during the late nineties by CEA (Commissariat à l'Energie Atomique) and IRSN (Institut de Radioprotection et de Sûreté Nucléaire), the advising body of the DGSNR (Direction Générale pour la Sûreté Nucléaire et la Radioprotection). This project was founded by the French nuclear industry together with the CEA and IRSN.

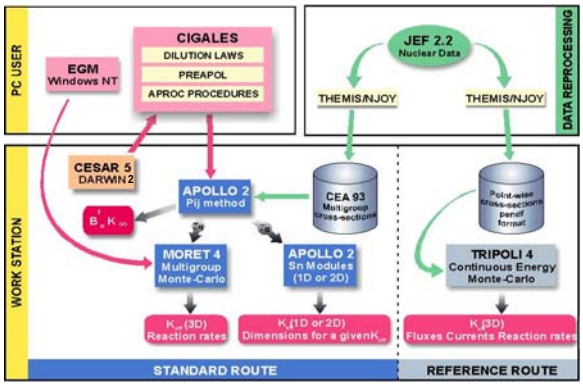

Figure 1**:**

The functional architecture of the CRISTAL code package, presented on Figure 1, is organized around two calculation routes:

- A "Standard route" or "Industrial route" with a multigroup formulation of cross-sections of the CEA93 library based on APOLLO2 computer code [2], a spectral computer code, and MORET 4 [3] computer code, a three dimensional Monte Carlo computer code.
- A "Reference route" based on TRIPOLI-4 computer code [4] with pointwise cross sections and continuous energy group.

These two calculation routes are using JEF 2.2, a basic microscopic cross library, via the CEA93 library with 172 energy group structure for the “standard route” and directly for the “reference route”.

This paper deals with the "Standard" route, the industry's preferred route for criticality safety evaluations.

The "Standard" route uses an input preprocessing Graphical User Interface, CIGALES [5]. CIGALES provides an efficient method to prepare APOLLO2 input decks and simplifies QA activities. Only basic "physical" data are used (fissile and structural media, shape, enrichment, dimension …). The APOLLO2 computer code performs cell or assembly spectrum calculations accounting for sophisticated self shielding process flux and macroscopic cross section determination. The resulting homogenized 172 group energy

structures are directly linked with the three-dimensional Monte Carlo code, MORET 4, which provides the capability to model simple or complex geometries.

The CIGALES computer code

The CIGALES computer code, a data generator used to provide in an interactive way the APOLLO2 assembly code data files for Pij and Sn calculations, was developed with Visual Basic and is available on Windows environment. The CIGALES computer code allows the atomic composition calculations of fissile materials using dilution laws and the generation of data for APOLLO2 calculations:

- for Pij calculations assigned to create macroscopic cross-sections (self-shielded, homogenised and/or collapsed) representing the chemical media used by the MORET 4 computer code (equivalent to media in homogeneous or heterogeneous geometries),
- for 1D and 2D calculations using the Sn method,
- for calculations of "criticality standards" (1D calculation with four predefined reflectors) with Sn method.

Moreover, the CIGALES computer code makes it possible to establish a coupling with the CESAR computer code (which is a simplified computer code for depletion calculations applied to the reprocessing).

The APOLLO2 computer code

The APOLLO2 computer code, developed since 1983 by CEA as a joint development effort with Electricité de France (EDF) and AREVA NP, makes it possible to solve the Boltzmann equation either with the integral form by the collision probability method (Pij, probability for a neutron created in volume Vi to have its first collision in volume Vj) or with the differential form by the Sn method. It also contains physical models to represent self-shielding effect, neutron leakage, double heterogeneity effect, non linear homogenization effect, etc. This modular computer code handles a great number of geometries (from the elementary cell in infinite medium to complex assemblies), and calculates in one and two dimensions the characteristic neutron parameters (such as cross-sections, buckling ...).

The MORET 4 computer code

The MORET computer code, developed since 1970 in the Criticality studies division at IRSN, is a neutron simulation code in three dimensions which uses the multigroup formalism for the cross-sections and the Monte-Carlo method to solve the Boltzmann equation. It allows us to determine the effective multiplication factor (keff) of any configurations more or less complex in three dimensions as well as reaction rates in the different volumes of the geometry and the leakages out of the system.

In the CRISTAL framework, the MORET computer code has benefited from intensive development and validation work. The improvement of the computing structure quality and the integration of new physical functionalities (anisotropic diffusion of neutrons and loosely coupled fissile units) led to the MORET 4 computer code.

3 APPLICATIONS TO A LOW ENRICHED URANIUM (LEU) UO2 FUEL FABRICATION PLANT

While an LEU fuel fabrication plant is processing enriched uranium lower than 6.6% 235U, the known enrichment bounding criticality risk for non-moderated fissile material, the various processes and production areas may not always remain water-free. Therefore, due to

moderation concerns, processes involving fissile material must be evaluated for criticality safety (normal and accident conditions).

The CRISTAL code package is well suited to handle criticality analyses.

The global fuel assembly fabrication route includes the following processes:

- UF6 UO2 conversion.
- UO2 powder storage.
- Pelletizing processes.
- Fuel assembly loading.
- Fuel assembly storage.

As far as criticality evaluations are concerned, some of these processes are controlled either by mass, concentration, geometry, storage pitch, neutron poison, or any combination of these listed controls.

Two examples of criticality control methods are provided on the following photos:

Figure 2**:** Pitch (Spacing) control

Figure 3**:** Safe layer (Safe slab) of fuel rods

Criticality Standards

Basic criticality data (i.e., criticality standards) are used as a first step in the determination of sub critical margins for all processes involving fissile materials. There are several worldwide criticality standards, e.g., ARH-600, which the US nuclear industry relies

on. Since 2003, the CRISTAL code package has been used to produce these basic safety values. Some important standard values for a UO2 fuel fabrication plant are given in the following tables where they are compared with older standards.

Table 1: UF6 – HF mixture

Minimal criticality parameter UF6-HF	Cylinder diameter (cm)	Spherical volume (l)	Uranium mass (kg)
SEC/T/77.70	50,4	200	115
CRISTAL (Sn)	46,2	156	98

Table 2: UO2F2 – H2O mixture

Minimal criticality parameter UO2F2 – H2O	Cylinder diameter (cm)	Spherical volume (l)	Slab thickness (cm)	Uranium mass (kg)
SEC/T/74.201	28,9	40	13,7	39
CRISTAL (Sn)	27,4	33	13,4	37,1

Table 3: UO2 – H2O mixture

Minimal criticality paramter Homogeneous UO2 – H2O	Cylinder diameter (cm)	Spherical volume (l)	Slab thickness (cm)	Uranium mss (kg)
CEA-N-2051	25,9	29,1	12	35,4
CRISTAL (Sn)	25,4	27	12,1	35,9

Actual configuration

As a consequence of the 1999 Tokai Mura criticality accident, the French safety authority implemented requirements for the reevaluation of several criticality safety items within the nuclear industry. One reevaluation included overloaded storage devices which were examined using CRISTAL. The same configuration was reproduced using MCNP and the results compared.

The configuration modeled is a typical infinite array of powder storage devices (Gemini) containing approximately 500 kg of low moisture content LEU UO2 per Gemini. Calculations demonstrate that even in the case of overloading these storage devices with 582 kg of LEU UO2 per Gemini, the configuration maintains a reactivity (Keff) lower than 1.0.

The computed configuration is shown Figure 2:

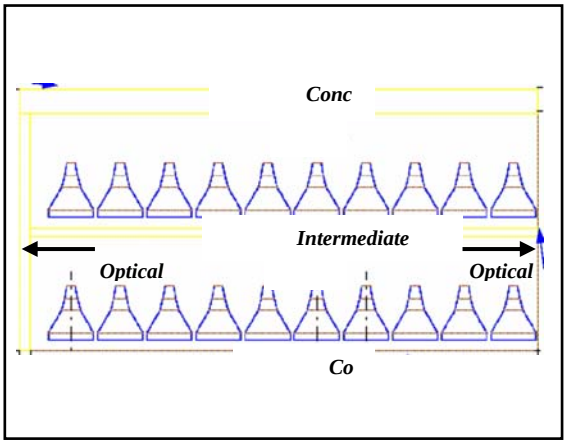

Figure 4**:**

Table 4 shows the main results of the CRISTAL code package compared with the MCNP results for the upper bounding cases.

Table 4: CRISTAL vs. MCNP results

		CRISTAL		**MCNP**	
Concrete water content (%)	**Water layer (cm)**	**Keff+3σ**	**σ (pcm)**	**Keff +I[+]**	**σ (pcm)**
8.9	**0.5**	0.903	232		
	1	0.918	234		
	1.5	0.916	245		
	2	0.897	231		
4.7	**0.5**	0.951	221		
	1	0.972	275	0.965	91
	1.5	0.962	245		
	2	0.936	243		
3.0	**0.5**	0.958	214		
	1	0.981	264	0.980	86
	1.5	0.979	256		
	2	0.960	248		

[+] Uncertainty I = 1.645 * sqrt($0.0065^2+\sigma^2$) where 0.0065 is derived from MCNP – JEF2.2 calculations

4 CONCLUSION

This paper demonstrates the capability of the CRISTAL code package to handle criticality safety concerns for the typical operation of a LEU UO2 fuel fabrication plant. The package uses sophisticated algorithms to solve the transport equation coupled with an up-to-date microscopic cross section set (JEF 2.2 level) produced by the APOLLO2 spectrum code. The three dimensional Monte Carlo computer code MORET4 allows the simulation of complex geometries encountered in production facilities. Finally, the Graphical User Interface, CIGALES, provides efficient preparation of the APOLLO2 input data and improves the QA process for the entire package.

REFERENCES

[1] The New CRISTAL Criticality-Safety Package
J.M. Gomit, P. Cousinou, A. Duprey, C. Diop, J.P. Grouiller, L. Leyval, H. Toubon, E. Lejeune
ICNC'99 Conference - Versailles - September 1999

[2] APOLLO2: a User-Friendly Code for Multigroup Transport Calculation
R. Sanchez, J. Mondot
Santa Fe Conference - April 1989

[3] MORET4: a Versatile and Accurate Monte Carlo Code for Criticality Calculation
A. Nouri, J. Dupas, A. Le Cocq, I. Bouilhac
ICNC'99 Conference - Versailles - September 1999

[4] A survey of TRIPOLI-4
J.P. Both, H. Derriennic, B. Morillon, J.C. Nimal
Proceedings of the 8th International Conference on Radiation Shielding - Arlington - Texas USA - April 1994

[5] The Graphical User Interface for the CRISTAL Package
E. Létang, G. Courtois, J.M. Gomit
ICNC'99 Conference - Versailles - September 1999

Optimizing Transport Security

Risk Analysis / Emergency Response Preparedness

Pascal Chollet
TN International (AREVA group)

ABSTRACT

The transport security is very important for AREVA group and the nuclear business in general. Because the transports are on the public field they are more sensitive for the persons and the environment.

In order to optimize the AREVA group transport security and the effective implementation of nuclear safety charters the Business Unit [BU] Logistics puts in place in 2006 a specific organization with a reinforced team and some new processes.

The scope is the transportation of nuclear materials and contaminated equipment representing a specific risk to the group (safety, physical protection, industrial and media)

The main BU LOGISTICS assignments are:

- to provide customized services to every BU of the group
- to certify and control external subcontractors chosen with BU's consent
- to supply all support for BU's in the field of:
  - Transportation preparation and organization
  - Emergency management
  - Monitoring of regulations
  - Technical expertise associated with transportation

This paper will introduce the approach of the risk analysis. The approach is in three steps:

- The transportation flow risk analysis,
- The Implementation priority
- The proposal for corrective actions.

For risks analysis, we evaluate, for each transportation flow, the occurrence or probability of an event during transport and the consequence of any potential event. From this, we get a risk level for each transport flow.

For the implementation priority, based on the risk level already evaluated in step 1, we evaluate and grade the current management of the risk. So, for each transportation flow, we have the risk level and the current level of the risk management.

For the last part we propose corrective actions for priority flows.

1 INTRODUCTION

The safe transport of radioactive materials has always been a priority concern for AREVA; today, and to meet tomorrow's challenges, working toward transport related risk reduction has become a major enterprise for AREVA which has entrusted its Logistics Business Unit to conduct this effort: AREVA's Transport Securization.

This paper describes in a first paragraph the context which has led the Logistics Business Unit to conduct transport securization. In a second part, the paper outlines the general principle that governed the designing of the organization in place supporting this effort. The last part describes the organization and methodology of the Logistics Business Unit transport securization

2 CONTEXT

Active in every stage of the fuel cycle, with actual production and manufacturing activities in 41 countries, and with two-third of its sales revenues depending on outside of France activities, the AREVA group manages numerous international streams of class 7 material between its plants as well as to and from other industrial plants worldwide.

Today, over 600 different steams of transports have been identified and are being part of the Logistics Business Unit transport securization perimeter. This number is increasing as nuclear renaissance springs around the globe. Indeed, AREVA faces increased demand for transportation, reaching out to new countries and regulations, involving new routes, new transport means, new actors within the logistical chain, and eventually new types of transport packages.

It is in this context, and to contribute to AREVA's sustainable worldwide growth, that the Logistics Business Unit efforts are being conducted.

3 GENERAL PRINCIPLES OF THE ORGANIZATION: CREATING A GLOBAL CENTRE OF EXCELLENCE

The predominant element that governed the designing of the organization in place for transport securization relates to human resources and their allocation to specific tasks at specific times. In an emergency situation, the organization shall allow for experts to be mobilized at any time of the day, any day of the year, and to be driven to efficiently work on their field of expertise. For that organization to be effective, it must be tested, feedback must be analyzed, and implemented back in the organization as needed. Simulation and training is therefore essential: training programs and large scale emergency response drills are specifically designed to improve methodology and effectiveness of experts involved in emergency situations. Good communication and harmonization of terminology are key factors of success when decisions are to be made in restricted timeframe.

Initiative was taken to create a dedicated organization implementing a series of actions aimed at reducing risks related to specific transports. Such organization is not only using existing local Logistics Business Unit resources and experience, but also seeking to use the advanced skills present in the nuclear market including AREVA entities worldwide.

The organization as described in the following paragraph structures the existing skills and expertise forming a harmonized global centre of excellence for nuclear logistics supporting safe, reliable, and efficient transportation of nuclear material and extending the actual safety records to face the challenges of nuclear renaissance.

4 ORGANIZATION AND METHODOLOGY: PREVENTING EMERGENCY SITUATIONS, MANAGING EMERGENCY SITUATIONS

Backed-up by over 30 years experience and comprised of a worldwide staff of over 800 employees fully dedicated to transport and package engineering, the Logistics Business Unit has designed and implemented its own methodology for preventing and managing emergency situations.

Four pillars support such methodology:

a) Control of Sub-contractors' Chain of Transports
b) Risk Analysis and Risk Management
c) Studies and Support
d) Emergency response

The first three pillars relate to preparedness for preventing any emergency situation, whereas the last one describes the organization in place to perform operational emergency response. All four are complementary and interdependent.

Control of Sub-contractors' Chain of Transports

Sub-contractors' control is achieved by implementing tight surveillance and an inspection program during transport on pre-qualified sub-contractors. Audits for qualification of sub-contractors are conducted by the Logistics Business Unit certified experts operating an active surveillance and backed-up by an inspection program of physical on-site checks at specific stages of the transport chain. Determination of the specific stages to be inspected and the periodicity of inspections are derived from the risk analysis performed for each transport stream. Inspection reports and their follow-ups feed back the risk analysis (described in the next paragraph); the risk analysis updates the inspection program, thus closing the cycle for a live continuous surveillance.

Risk Analysis and Risk Management

The Logistics Business Unit conducts a risk analysis on every AREVA transport stream. Following the risk analysis, proper recommendations are elaborated for reducing such risks.

The risk analysis establishes the probability of occurrence of an event during transport and the impact of such events on AREVA activities. Transport related events can be attributed to impacting safety, security, the media, or industrial streams.

Combining occurrence and impact provides ground for defining the risk level and the priority of action to engage on recommendations for lowering the risk. Recommendations range from technical solutions involving the development of new transport routes, packages, transport means, tie-down systems, modes of transport, but also improved fleet management, logistics, industrial partnership, processes, training, etc..

Studies and Support

The Logistics Business Unit's organization for transport securization provides support and expertise in fields such as:

- Alternative transport routes
- Public acceptance
- Emergency procedures and operations
- Sustainable development in the field of transport
- Large scale logistical studies
- Package licensing strategy
- Package fleet management
- Public acceptance
- Training,
- Tracking systems
- Tie-down systems
- etc.

Emergency Response

One of the principles among those developed by the IAEA for the safe transport of radioactive material is that emergency preparedness enables to reduce the radiological consequences to persons and the environment, in case of accident.

The IAEA Regulations for the Safe Transport of Radioactive Material require that emergency provisions, as established by relevant national organizations, shall be observed to protect persons, property and the environment.

To help public authorities in charge of emergency response to establish adapted emergency plans, the IAEA published a Safety Guide. This Safety Guide was published for the first time in 1988. The current edition was published in 2002 under the reference TS-G-1.2.

In France, the prefect of the department where the accident occurs is responsible for decisions and measures required to ensure the protection of both population and property at risk.

During an accident, the ministers concerned provide the prefect with recommendations and information, in order to help him make the proper decisions.

The nuclear industry and transport companies also have to be prepared to intervene and to support the authorities at their request, depending on their specialities and their capacities.

The Logistics Business Unit emergency response organization is aimed at reducing transport related risks for the AREVA Group as well as at supporting authorities in the fields of packaging, transport means, contamination and irradiation risk evaluation, proximity expertise and evaluation (with its on-site mobile technical team), and communication.

Emergency preparedness is about providing decision makers with timely and reliable information. For that purpose, the organization provides for the joint effort of both the technical team and the communication team. Making the right decision shall be based on a very quick estimation of the potential consequences of the accident. To be able to evaluate such consequences, a good knowledge of the particular transport, accidental conditions, and material being transported is essential (drop, fire, immersion, duration of the accident, area with impact on the population and the environment).

The organization efficiency is measured against its capacity to achieve the objective of returning under safe conditions. At an early stage, scenarios for recovery of the damaged packages are elaborated by the technical team. Confirming the safety of the packages is a prerequisite to finalizing the recovery scenarios.

Data must be checked prior to release and communication. Communication should allow for simple and clear messages utilizing a harmonized terminology which must be established in advance and tested.

To prepare the emergency teams properly and acquire effective emergency plans, the Logistics Business Unit has been actively participating to regular training exercises with various ministerial department, the nuclear industry, members of the public and the media. Feedback from such training exercises is taken into account to improve the emergency procedures.

The table 1 below summarizes the last large scale national drills performed with the Logistics Business Unit.

Table 1 : Crisis exercises performed with the Logistics Business Unit

	2002	2003	2004	2005	2006	2007
Materials transported	**Research used fuel**	**Low level waste**	**Used fuel and MOX used fuel**	**Liquid waste**	**Enriched UF_6**	**Alpha technological wastes**
Transport means	**Road**	**Road**	**Rail**	**Road**	**Road**	**Road**
Packaging	**IU 04**	**DV 78**	**TN 12**	**TN CIEL**	**30B cylinder**	**RD26**
Transport company	**LEMARECHAL CELESTIN (LMC)**	**LEMARECHAL CELESTIN (LMC)**	**SNCF**	**LEMARECHAL CELESTIN (LMC)**	**LMC**	**LMC**
Shipper	**CEA Saclay center**	**AREVA NC La Hague plant**	**EDF Chinon NPP**	**EDF Paluel NPP**	**EURODIF**	**MELOX**
Consignee	**AREVA NC Cadarache**	**Centraco incineration plant**	**AREVA NC La Hague**	**Centraco incineration plant**	**GNF**	**LANL**
Transport agent (commissionning)	**TN International**	**TN International**	**TN International**	**TN International**	**TN International**	**TN International**
Area	**Yonne (Auxerre)**	**Eure-et-Loire (Chartres)**	**Indre-et-Loire (Tours)**	**Val d'Oise (Cergy-Pontoise)**	**Roanne (Loire)**	**Montoir (Loire Atlantique)**

Feedback from each training exercise or actual emergency situation often relates to improving communication and reactivity. Feedback has been very beneficial and has largely influenced the actual transport securization organization.

CONCLUSION

AREVA has engaged in a major enterprise for transport related risk reduction to sustain its worldwide growth and properly manage increasing transport activities induced by nuclear renaissance.

A dedicated organization was created, tested, and improved, leading to an effective centre of excellence for nuclear logistics supporting safe, reliable and efficient transportation of nuclear material.

COMPARISON OF THE SEVERE ACCIDENT BEHAVIOUR OF ADVANCED NUCLEAR FUEL ROD CLADDING MATERIALS

M. Grosse, L. Sepold, M. Steinbrueck, J. Stuckert

Forschungszentrum Karlsruhe (Karlsruhe Research Center, Germany)
Institute for Materials Research; Hermann-von-Heelmholtz-Platz 1, D-76344 Eggenstein-Leopoldshafen, Germany
Mirco.Grosse@IMF.FZK.de, Leo.Sepold@IMF.FZK.de
Martin.Steinbrueck@IMF.FZK.de, Juri.Stuckert@IMF.FZK.de

N. Ver
AEKI Budapest
Konkoly Thege Miklos 29-33, 1121 Budapest, Hungary
nver@aeki.kfki.hu

ABSTRACT

The isothermal and transient oxidation behaviour of the four widely used cladding materials, the Zr-Sn alloys Zry-4 and DUPLEX and the Zr-Nb alloys E110 and M5 in steam, oxygen and air were investigated. The oxidation kinetics at temperatures above 1050°C is similar for these materials. Parabolic time dependences of mass increase and oxide layer growth were found. The oxidation rates depend on temperatures by Arrhenius functions. The activation energies differ for the different zirconium oxide crystal structures. At lower temperatures the behaviour can strongly differ between the materials due to the so called “breakaway effect”. In the temperature range between 800 and 1000°C this effect was found for oxidation of E110 in steam and oxygen. At 1000°C the oxidation of Zry-4 shows this effect, too. It results in an enhanced oxidation. The time dependence changes from parabolic to nearly linear. For the D4 layer of the DUPLEX material and for M5 no breakaway takes place under the conditions applied. The effect was also found for transient oxidation of E110 with heating rates below 0.1 K/s. For these low heating rates the time in which the materials are in the temperature range where the breakaway effect takes place is long enough for enhancing oxidation. The strong influence of spalling of oxide layers on the severe accident behaviour of fuel rod bundles can be seen by comparison of the large scale bundle simulation tests QUENCH-6 and QUENCH-12. The hydrogen release of the QUENCH-12 bundle during reflooding, where massive spallation of oxide parts took place, was six times higher than of the QUENCH-6 bundle under comparable conditions. Oxidation in air shows faster kinetics than in pure oxygen or steam. The reaction depends nearly linear on time. It is caused by the formation of a very porous oxide scale mixed with zirconium nitride which is formed under (local) oxygen starvation conditions, e.g. at the phase boundary between oxide and metal.

1 INTRODUCTION

Advanced cladding materials were developed for longer operation times in nuclear power plants and extended burnup of the fuel elements. They are optimized regarding their corrosion behaviour under operational conditions and were also tested for LOCA (loss of coolant accident) and RIA (reactivity-initiated accident) conditions by the manufacturers. However, also the oxidation behaviour at severe accident conditions (accidents beyond the loss of coolant accident LOCA) has to be known to prove the safety under these circumstances and to improve models used in severe accident simulation codes. Basis of the investigations are loss of coolant and reflooding scenarios.

The overheated cladding material reacts rapidly with steam at high temperatures. Simplified it can be described by:

$$Zr + 2\ H_20 \rightarrow ZrO_2 + 2\ H_2 + 596\ kJ \quad (1)$$

It is a strongly exothermic reaction which causes additional increase of temperature in the reactor. The steam oxidation results in degradation of the metallic cladding material and in release of a large amount of hydrogen.

In contrast to the classical Zircaloy-4 (Zry-4) which is extensively investigated over a wide temperature range from operational conditions to temperatures beyond design basis accident [1], the publicly available data on high temperature oxidation of the various advanced cladding materials is scarce.

2 MATERIALS AND EXPERIMENTS

2.1 Materials

The investigations comprise two Zr-Sn alloys (D4 layer at the DUPLEX cladding and Zry-4) and two Zr-Nb alloys (E110 and M5). Whereas Zry-4, M5 and E110 are homogeneous materials, the DUPLEX material consists of a Zry-4 bulk and a D4 protection layer (thickness 150 µm) at the outer surface. The D4 layer differs from Zry-4 mainly by a reduced tin content and a higher concentration of iron and chromium. The main difference between the both Zr-Nb alloys is the higher iron content in M5. The concentrations of the main alloyed elements in the investigated materials are given in Table 1.

alloy	Sn	Nb	Fe	Cr	O
E110	< 0,04	1,00	< 0,01	<0,003	0,05
D4	0,50	0,0001	0,50	0,20	0,14
M5	< 0,03	1,00	0,34	0,04	0,14
Zry-4	1,50	0,0001	0,21	0,10	0,14

Table 1: Chemical composition of the cladding alloys, Zr - balance

2.2 Separate-Effect Tests

For the separate-effect tests different facilities were used: a thermo-balance with two furnace frames, one for reaction in oxygen or air with maximal temperature of 1600°C and one for steam oxidation with maximal temperature of 1100°C, and a horizontal tube furnace

for isothermal oxidation in steam. For the tests segment with a length of 10 or 20 mm were cut from original cladding tubes.

The specimen has to put into the thermo-balance at room temperature, then it was heated in flowing Ar atmosphere. When the test temperature (isothermal tests) or start temperatures (transient test) were reached the injection of the oxidizing gas and the mass registration was started. After the pre-defined oxidation time the injection of the reaction gas was finished and the specimen was cooled down to room temperature in flowing Ar.

The horizontal tube furnace provides the possibility of loading the specimen into the furnace at test temperature in flowing Ar atmosphere. After some seconds for temperature homogenisation the test gas injection starts. Reducing (H_2), inert (Ar, He) or oxidizing (air, O_2, steam and mixtures) atmospheres can be applied. The off-gas composition was measured with the mass spectrometer "GAM 300". After the test the specimen can be cooled down to room temperature in Ar within about five minutes.

2.3 Large-Scale Bundle Tests

Quench experiments with overheated nuclear fuel rod bundle simulators were applied to study the behaviour of the reactor core during reflooding in various LOCA or severe accident scenarios. The vertical mounted fuel rod simulators have a length of 2500 mm. A part of them are electrical heated. Up to now 13 QUENCH-experiments were performed; differing in their accident scenario (e.g. air ingress, boil-off, slow cooling), in the applied reactor geometry and in the applied cladding materials including different types of control rods.

The QUENCH-12 experiment [2] was carried out to investigate the effects of VVER materials (niobium-bearing alloys) and bundle geometry on core reflood, in comparison with test QUENCH-06 using Western European PWR simulator bundle (Zircaloy-4) [3]. QUENCH-12 was conducted with largely the same protocol as QUENCH-06 given in Fig. 1, such that the effects on the VVER characteristics could be observed more easily.

While the PWR bundle uses a single unheated rod, 20 heated rods, 1 unheated central rod and 4 corner rods arranged on a square lattice, with a heated length of 1000 mm, the VVER bundle uses 13 unheated rods, 18 heated rods and 6 corner rods, arranged on a hexagonal lattice. The coolant channel area ratio between two bundles is QUENCH-12/QUENCH-06 = 1.09, therefore the fluid flow rates were preset 9 % higher for the QUENCH-12 bundle than for the QUENCH-06 bundle to provide the same flow velocity.

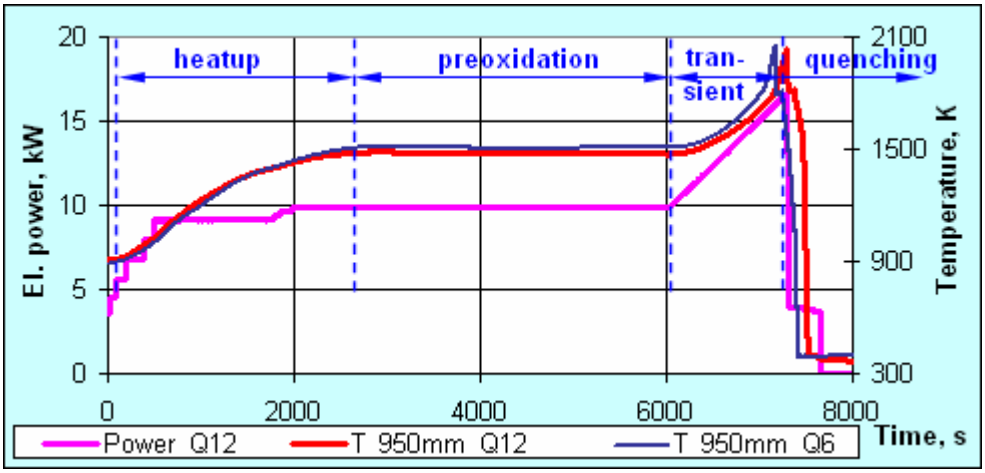

Figure 1: Temperature at the 950 mm elevation and electric power vs. time together with an indication of test phases

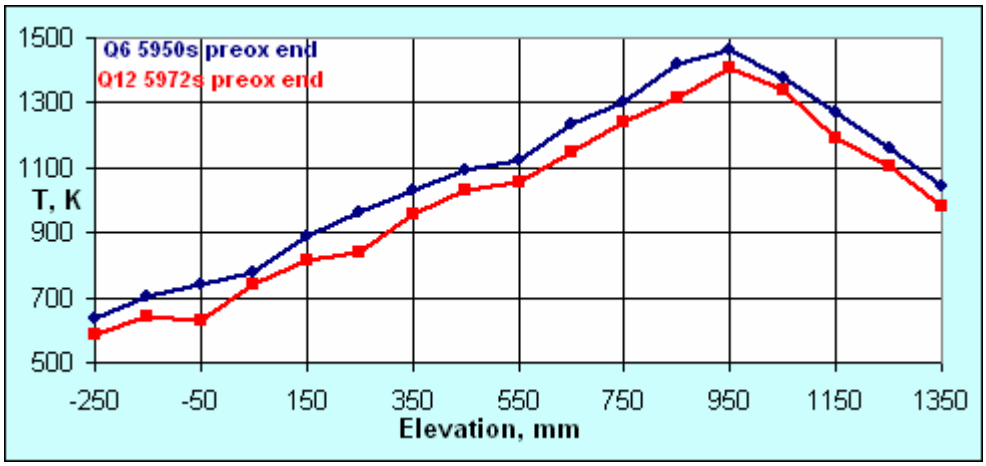

Figure 2: Axial temperature distribution at the end of pre-oxidation phase

The bundle material mass ratio is QUENCH-12/QUENCH-06 ~ 0.97, however the metallic surface ratio is QUENCH-12/QUENCH-06 = 1.22. In this connection the electrical power for the QUENCH-12 bundle was installed lower than for the QUENCH-06 bundle to compensate the higher chemical energy production due to exothermic steam-metal reaction.

The steam, ascending from the bundle bottom, is heated and produced a pronounced axial temperature profile. The axial temperature distribution during the pre-oxidation phase given in Fig. 2 shows that the greater part of the QUENCH-12 bundle was oxidised long period at temperatures between 1000 K and 1300 K, i.e. under conditions typical for breakaway oxidation (see below) of the E110 alloy.

3 RESULTS AND DISCUSSION

3.1 Isothermal Oxidation Behaviour

3.1.1 Steam oxidation

The oxidation of all materials can be described by the parabolic time dependences expected for diffusion controlled reactions for all temperatures investigated at least for short oxidation periods:

$$\Delta m, D_{oxide} = \delta_{m,D} \cdot \sqrt{t} \quad (2)$$

Δm is the mass increase per surface area, D the oxide layer thickness. δ_m and δ_D are the mass increase rate and the oxide layer growth rate, respectively. As an example, Fig. 3 gives the time dependence of the relative mass increase during steam oxidation at 900, 1000, 1100 and 1400°C for the four materials investigated. Because the oxidation occurs at both, inner and outer surfaces, the mass increase of the DUPLEX material is a result of oxidation of D4 and Zry-4 at outer and inner surface, respectively.

In Fig. 4 the temperature dependences of the mass increase rate and of the oxide layer growth rates are given for the investigated materials. The time dependences of oxidation rate δ for each material can be described by two Arrhenius functions, valid for the monoclinic (lower temperatures) and tetragonal (higher temperatures) ZrO_2, respectively:

$$\delta_{m,D} = \delta^{*}_{m,D} \cdot e^{\frac{Q}{RT}} \quad (3)$$

Q is the activation energy and R the universal gas constant (8.314 J mol^{-1} K^{-1}). For comparison the Leistikow – Schanz and the Cathcart – Pawel correlations [4] are given in the diagrams. They better describe the behaviour of the Zr – Nb alloys than of the Zr – Sn alloys.

Tab. 2 gives the activation energies determined for all investigated materials at the lower and the higher temperature ranges. The transition temperature between the monoclinic and tetragonal ZrO_2, is about 50 K higher for the both Zr – Nb alloys than for the Zr – Sn alloys. Due to the low oxide layer thicknesses at temperatures below this transition (only several microns), the uncertainties in the metallographic determination of the thicknesses are high. Therefore a certain determination of the activation energies for the oxide layer growth is not possible.

At 1400°C the oxidation behaviours of the four materials are quite similar. The oxidation of the Zr – Nb alloys is slightly faster than of the Zr – Sn alloys. Due to the higher activation energies of the Zr – Nb alloys the situation changes at temperatures between 1000 and 1200°C. In this temperature range the oxidation rate is lower for the Zr - Nb alloys than Zr - Sn alloys. With increasing temperature the oxidation behaviour of the D4 layer converges towards the higher oxidation rate of Zry-4. Reason for this convergence is the diffusion of tin from the Zry-4 bulk into the D4 layer which is relative fast, at least at temperatures of 1200°C and higher.

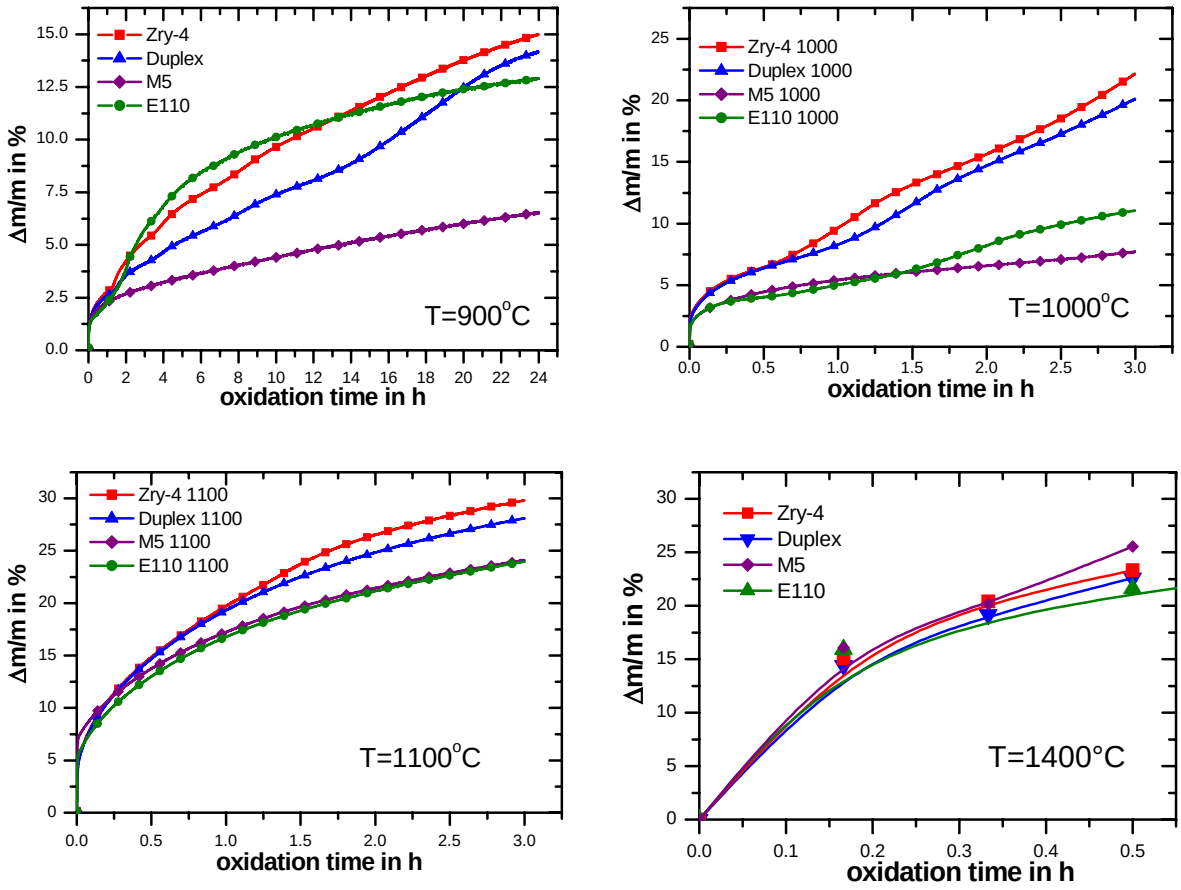

Figure 3: Comparison of the time dependence of the relative mass increase during steam oxidation of the materials Zry-4, Duplex, E110 und M5 at 900, 1000, 1100 and 1400°C

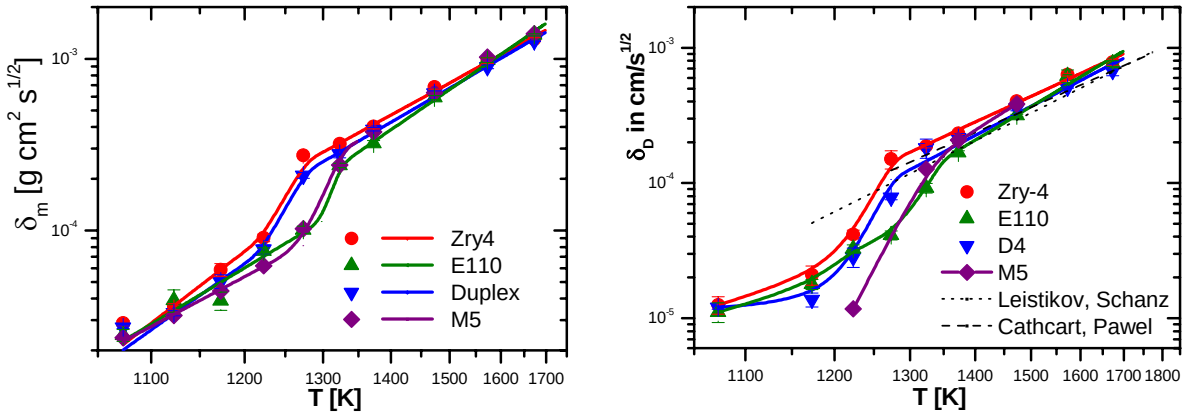

Figure 4: Temperature dependence of mass increase rate δ_m and oxide layer growth rate δ_D of the investigated materials

Fig. 5 shows the tin concentration profile after 3 h annealing at 1100°C in flowing argon. The profile was determined by X-ray fluorescence measurements with a beam size of 8 µm at the FLUO/TOPO beamline of the synchrotron source ANKA of FZ Karlsruhe. The diffusion rates in the DUPLEX material determined for temperatures between 1000 and 1400°C are significantly higher than the values given in [5] for pure zirconium. On the other hand the activation energy for tin diffusion is in the DUPLEX material significantly lower than the value given in [5] (DUPLEX: 138 kJ/mol, zirconium [5]: 212 kJ/mol). A detailed description and discussion of the results will be given in [6].

At 1000°C the oxidation rates of D4 and Zry-4 differ significantly. Reason is the breakaway effect, discussed below, which occurs in Zry-4 but not in the D4 layer. At lower temperatures the D4 layer shows its protective behaviour against oxidation. At these temperatures tin diffusion does not affect the oxidation rate significantly.

The slowest oxidation takes place in M5. The oxidation in E110 is enhanced between 800 and 950°C also at early times for which the parabolic kinetics is valid. Possibly, the beginning of the breakaway effect results in a faster oxidation.

material	temperature range	mass increase	oxide layer growth
Zry-4	800°C ≤ T < 950°C	$\delta_m^{Zry-4} = 2.857 \cdot e^{-12655\,K/T}$	not to be determined
	1000°C ≤ T ≤ 1400°C	$\delta_m^{Zry-4} = 0.298 \cdot e^{-9033.3\,K/T}$	$\delta_D^{Zry-4} = 0.213 \cdot e^{-9277.1\,K/T}$
Duplex/D4	800°C ≤ T < 950°C	$\delta_m^{Duplex} = 1.114 \cdot e^{-11718\,K/T}$	not to be determined
	1000°C ≤ T ≤ 1400°C	$\delta_m^{Duplex} = 0.409 \cdot e^{-9614.4\,K/T}$	$\delta_D^{D4} = 0.398 \cdot e^{-10472\,K/T}$
E110	800°C ≤ T < 1000°C	$\delta_m^{E110} = 0.240 \cdot e^{-9945.6\,K/T}$	not to be determined
	1050°C ≤ T ≤ 1400°C	$\delta_m^{E110} = 1.263 \cdot e^{-11332\,K/T}$	$\delta_D^{E110} = 1.149 \cdot e^{-12070\,K/T}$
M5	800°C ≤ T < 1000°C	$\delta_m^{M5} = 0.080 \cdot e^{-8770.6\,K/T}$	not to be determined
	1050°C ≤ T ≤ 1400°C	$\delta_m^{E110} = 0.623 \cdot e^{-10170\,K/T}$	$\delta_D^{M5} = 1.149 \cdot e^{-12070\,K/T}$

Table 2: Parameter of the Arrhenius temperature dependence of mass increase and oxide layer growth

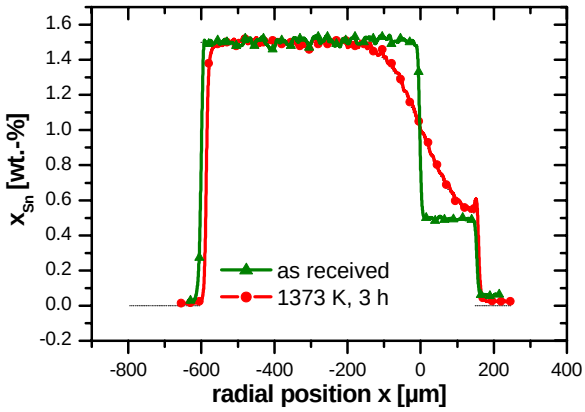

Figure 5: Tin concentration profile in DUPLEX cladding in the as-received state and after 3 h annealing at 1100°C in inert atmosphere

The parabolic oxidation kinetics is typical for reactions were oxygen has to diffuse through a growing oxide scale. The oxidation time dependences of E110 in the temperature range between 800 and 1000°C and of Zry-4 at 1000°C (see as examples Fig. 6) differ from the parabolic behaviour. At later times (4h for E110 at 800°C, 1 h for Zry-4 at 1000°C) the oxidation is enhanced. The oxidation kinetics changes from parabolic to nearly linear.

Differences from the parabolic time dependence of the mass increase of the DUPLEX material are caused by the oxidation of the inner (Zry-4) surface. For M5 only parabolic behaviour was found at all temperatures investigated.

The reason is the so called ”breakaway effect”. Due to lattice coherence and fitting stresses to the metal the oxide growth starts with an under-cooled tetragonal micro-structure. After a certain oxide layer thickness is reached a martensitic transformation from tetragonal to monoclinic oxide occurs. This transformation is connected with volume change and formation of residual stresses, micro cracks in hoop direction (see Fig. 7) and spalling of oxide parts, as shown in Fig. 6. The oxide layer looses its protective effect against further oxidation. Steam can penetrate into the cracks and the oxidation is no longer controlled by the diffusion of oxygen through the ZrO_2 scale.

Breakaway of oxide layer parts was found for E110 specimens after oxidation at a wide temperature range of 800 to 1000°C, for Zry-4 only at 1000°C. For M5 and D4 no breakaway is found at the temperatures and times investigated. Here the higher content of iron and chromium containing second phase particles increases the mechanical stability of the oxide layers.

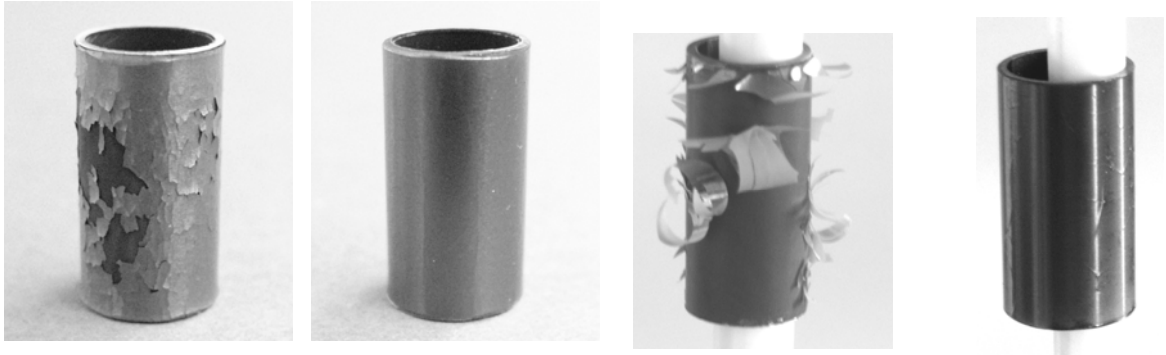

Zry-4, 1000°C, 2h Duplex, 1000°C, 2h E110, 800°C, 4 h M5, 800°C, 4 h

Figure 6: Comparison of oxide appearance after steam oxidation with and without breakaway effect

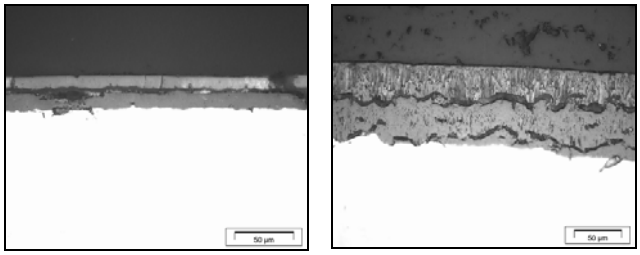

E110, 1223 K Zry-4, 1273 K

Figure 7: Oxide layer morphology after 1 h oxidation

The morphology of the oxide layer parts spalled differs significantly between E110 and Zry-4. For E110 these layers are finer than for Zry-4. Layer thicknesses of about 5 - 10 µm were found for E110, for Zry-4 of 30 – 50 µm.

3.1.2 Air oxidation

Actually, various scenarios have attracted interest in which the fuel rods are prone to exposition in air-containing atmospheres. Presence of air increases to the risk of an accelerated escalation basically due to stronger heat released in Zr oxidation; and additionally causes the formation of uranium oxide phases with lower melting temperature and of more volatile oxidic fission products (such as ruthenium oxides). An exemplary scenario could arise under shutdown conditions when the reactor coolant system is open to the containment atmosphere.

Systematic investigations on air oxidation under such conditions were performed by parametric separate-effects tests in the temperature range 800-1500°C [7]. These findings were cross-checked for its applicability to the outcome of the large-scale bundle test QUENCH-10 on air ingress performed in 2004 [8].

Fig. 8 shows the typical parabolic oxidation kinetics of Ziraloy-4 in oxygen caused by the growing compact oxide scale which acts as a diffusion barrier. The reaction kinetics in nitrogen is also of the parabolic type, but by orders of magnitude lower as compared to

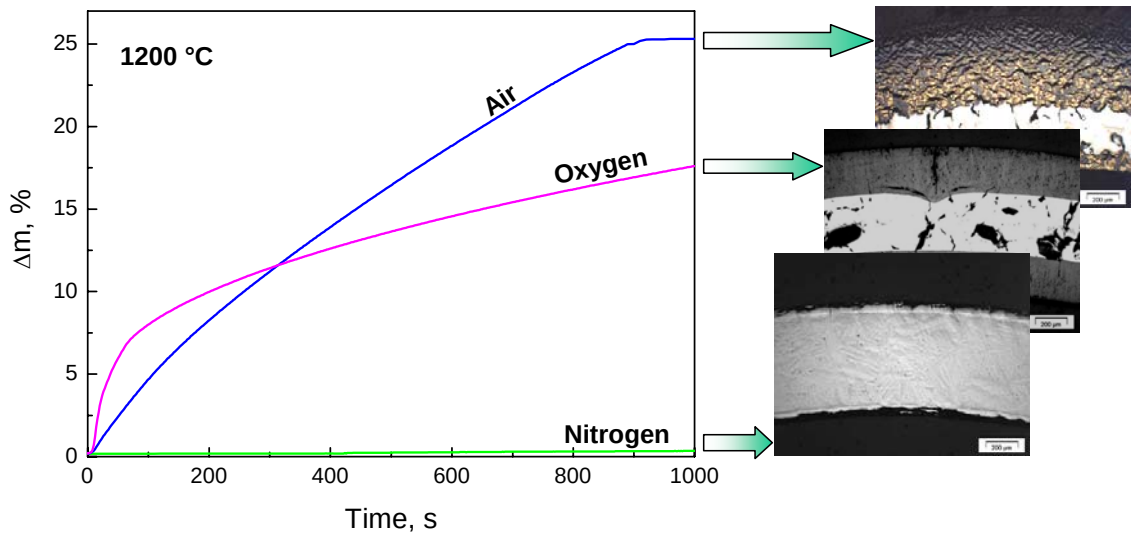

Figure 8: Reaction of Zircaloy-4 cladding segments in oxygen, nitrogen, and air: Mass gain as indicator for reaction rates and metallographic images.

oxygen.

The mixture of both gases, i.e. air, gives a much faster kinetics of a linear character. This is caused by the formation of a very porous oxide scale mixed with zirconium nitride (gold-coloured phase) which is formed at the phase boundary oxide-metal.

Similar studies on the oxidation of Zircaloy-4 in mixed air-steam and nitrogen-steam atmospheres and on the influence of pre-oxidation in steam on subsequent reaction in air and nitrogen confirmed the significant effect of nitrogen onto cladding oxidation and degradation under the conditions of a severe accident, although oxide formation is thermodynamically favoured.

This can be explained by the role of nitride phases which are formed under oxygen starvation conditions. The nitride is re-converted into oxide under returning oxidising conditions. The strong degradation seen in many of the experiments is due to the significantly different densities of ZrO_2 and ZrN.

Regarding modelling of air ingress in severe accident computer codes, it is suggested that parabolic correlations for oxidation in air should be applied only for high temperatures (>1400 °C) and for pre-oxidised cladding (≥ 1100 °C). For all other conditions, faster reaction kinetics is more appropriate.

3.2 Transient Oxidation Behaviour

In order to prove the possibility of the breakaway effect under transient conditions a limited number of oxidation tests in steam with varying heating rates between 0.05 - 0.3 K/s were performed. Start and end temperature were 400 and 1100°C, respectively.

Oxide breakaway was found in the transient tests only for E110. Spalled oxide layer parts are visible for all applied heating rates as Fig. 9 shows. At heating rates < 0.1 K/s the oxidation is accelerated significantly inside breakaway temperature region, as demonstrated in Fig. 10. The broken line indicates the time dependence to be expected for parabolic behaviour.

Transient tests in oxygen up to 1580 °C have been additionally conducted in a thermal balance. Starting temperatures of oxidation were 1100 °C and room temperature to examine transient oxidation excluding and including the breakaway region, respectively.

Fig. 11 compares the oxidation rates of four alloys in transient tests from 1100 °C. Heat up to 1100 °C was in inert atmosphere. At a first glance the curves look similar. As was seen in the 1100 °C isothermal tests, the niobium-bearing alloys show a slightly favourable behaviour during the initial period of the transient tests.

0.05 K/s 0.10 K/s 0.20 K/s 0.30 K/s

Figure 9: Post test appearance of E110 specimens after transient oxidation at various heating rates.

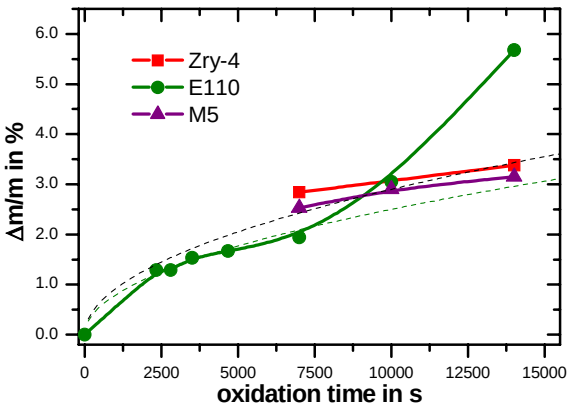

Figure 10: Relative mass increase during transient oxidation tests in steam

At about 1300 °C the situation changes and the tin alloys exhibit slower oxidation rates. The reaction rates of the tin and niobium alloys among themselves are very similar. At about 1480 °C the reaction rates significantly increase for all alloys. The reason for this behavior will be discussed later.

The picture is slightly different for the test series starting with oxidation from room temperature as can be seen in Fig. 12. Although the temperature program was identical for the four experiments (shown by the dotted curves in Fig. 12), the resulting TG curves look less similar to each other than those from in the isothermal series. Again, the tin alloys reveal very similar oxidation kinetics over the whole temperature range. The E110 curve starts to show irregularities at 930 °C, but recovers at 1100 °C. The highest oxidation rates for the mid temperature region are measured for M5, the lowest for E110. This relation reverses above 1480 °C.

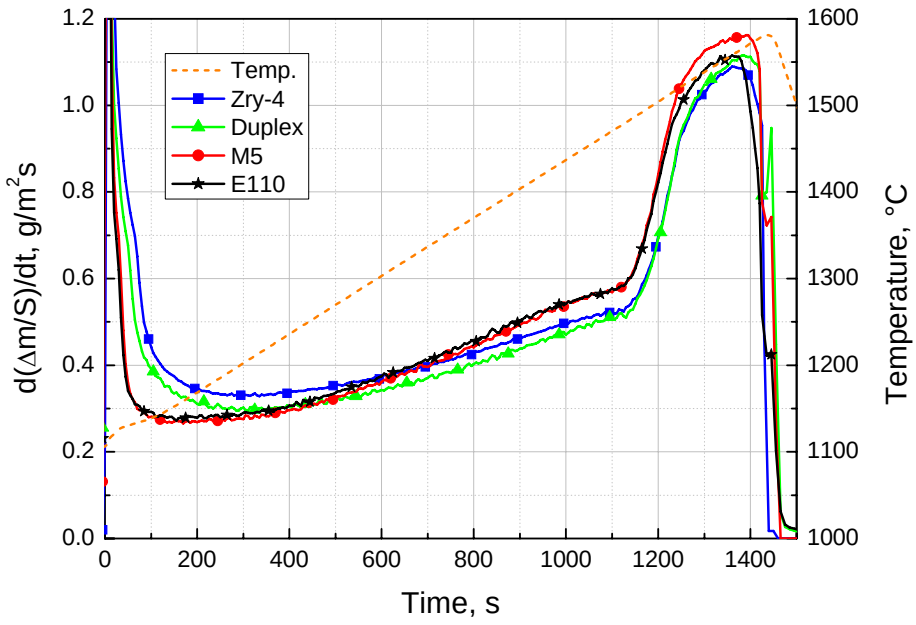

Figure 11: Reaction rate vs. time during transient oxidation of zirconium alloys in oxygen from 1100 to 1580 °C

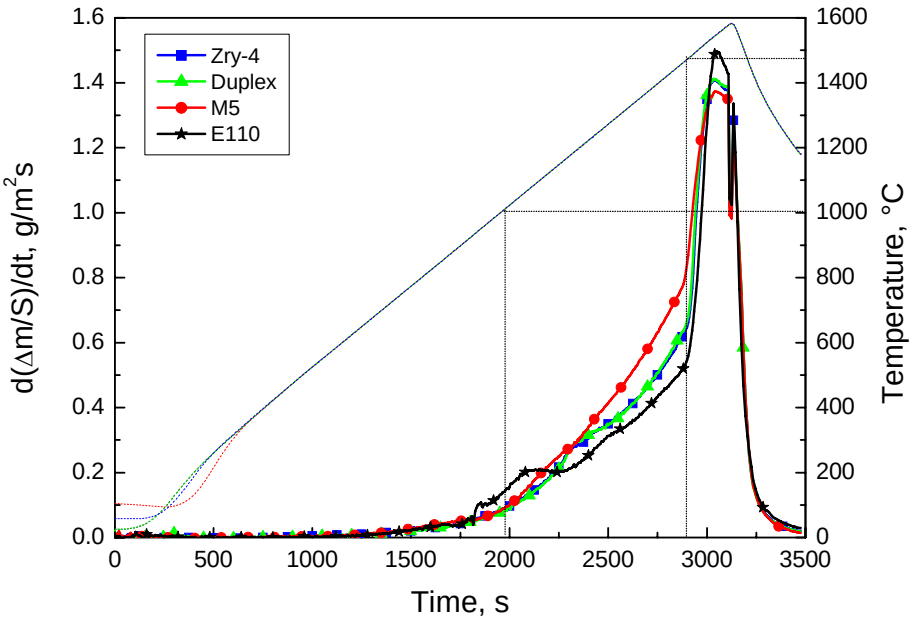

Figure 12: Reaction rate vs. time during transient oxidation of zirconium alloys in oxygen from room temperature to 1580 °C

Generally, three domains can be distinguished in the diagram. The increase in reaction rates with temperature reveals inhomogeneities, i.e. bends in the TG curves, at about 1000 °C and identically to the first series at 1480 °C, as indicated by the dotted lines in Fig. 12. The three domains are related to the three crystallographic modifications of the zirconium oxide scale, namely monoclinic, tetragonal, and cubic.

3.3 Bundle Simulation Tests

The examination of the VVER bundle QUENCH-12 with E110 cladding revealed significant differences compared to the reference test QUENCH-06 with Zricaloy-4 cladding.

The first corner rod D of the QUENCH-12 bundle, which was withdrawn at the end of the pre-oxidation phase, revealed an extensive breakaway oxidation along the complete hot zone. It was not possible to measure the oxide layer thickness due to spalling of the oxide scales (Fig. 13). The second corner rod F was withdrawn during the transient phase before starting the moderate temperature escalation. This rod also exhibited an extensive spalling of oxide scales.

The QUENCH-12 bundle was investigated in detail by videoscope before filling with epoxy resin (Fig. 14). Axial differences in the surface morphology were observed. The lowest elevation, where breakaway oxidation of Zr1%Nb-cladding surface took place, was at 400 mm. The maximum temperature at this bundle position was about 850°C. The formation of typical breakaway oxidation at the relatively cooler Zr2.5%Nb-shroud took place at higher elevations.

Figure 13: QUENCH-12, the withdrawn corner rods D and F revealed breakaway oxidation with intensive spalling of oxide scales

Figure 14: QUENCH-12, videoscope observation at the 650 mm elevation

It should be mentioned that the findings on breakaway effect of the VVER-type cladding material reported in this section refer to long term oxidation at temperatures between 730 and 1030°C. Such scenarios are more applicable for accident conditions for spent fuel pool than for reactor accidents.

The initially coarse shroud surface revealed thicker spalled oxide scales, but the oxide sub-layer showed the regular dark structure similar to the oxide inner sub-layer on the cladding surface.

The shroud surface showed at the higher hottest elevations a nodular kind of breakaway oxidation, whereas there is no evidence of breakaway on the cladding surface at these elevations. However the formation of longitudinal and circumferential cladding cracks in the hot bundle zone (0.70-1.00 m) is typical for Zircaloy-4 cladding as well.

Post-test metallographic investigations of the QUENCH-12 bundle showed an influence of the breakaway effect with extensive spalling of oxide scales at rod claddings and shroud at elevations higher than 400 mm. No influence of the breakaway effect was observed for the QUENCH-06 bundle (Fig. 15).

It is interesting to note that the surface of claddings of the QUENCH-12 bundle showed more regular and homogeneous structure of the oxide layer than the surface of the solid corner rods of this bundle. Both surfaces show breakaway oxidation being more pronounced at the corner rods. One possible reason for it could be the different mechanical properties of cladding tubes and solid corner rods.

Measurements of hydrogen production during the QUENCH-12 test are as follows: 34 g were released during the pre-oxidation and transient phases and about 24 g in the quench phase. The amount released in the quench phase is six times higher than in QUENCH 06 with about 4 g (Fig. 16). The reasons for the increased hydrogen production may be extensive damaging of the cladding surfaces due to the breakaway oxidation, local melt formation with subsequent melt oxidation, and the release of hydrogen previously absorbed by the metal. The hydrogen absorbed by claddings was measured by the hot extraction method (long heating of 2 cm probes by 1500 °C). This measurement showed higher concentration of absorbed hydrogen for the Zr1%Nb claddings in comparison to the Zry-4 claddings (Fig. 17).

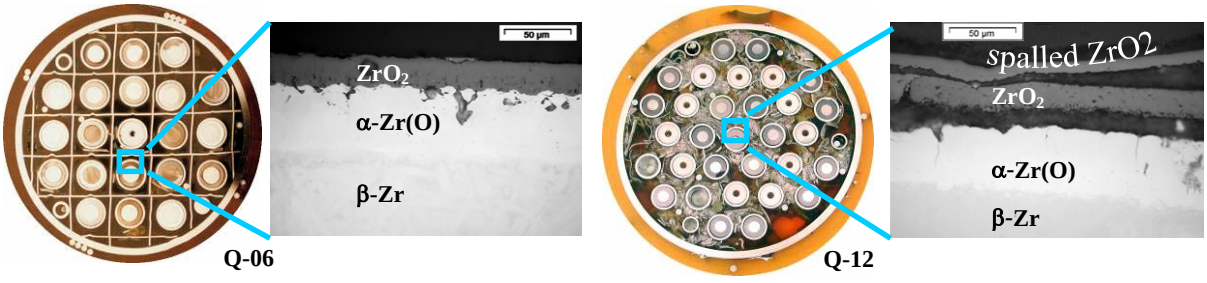

Figure 15: Comparison of cross-sections of QUENCH-06 and QUENCH-12 bundles at the 550 mm elevation.

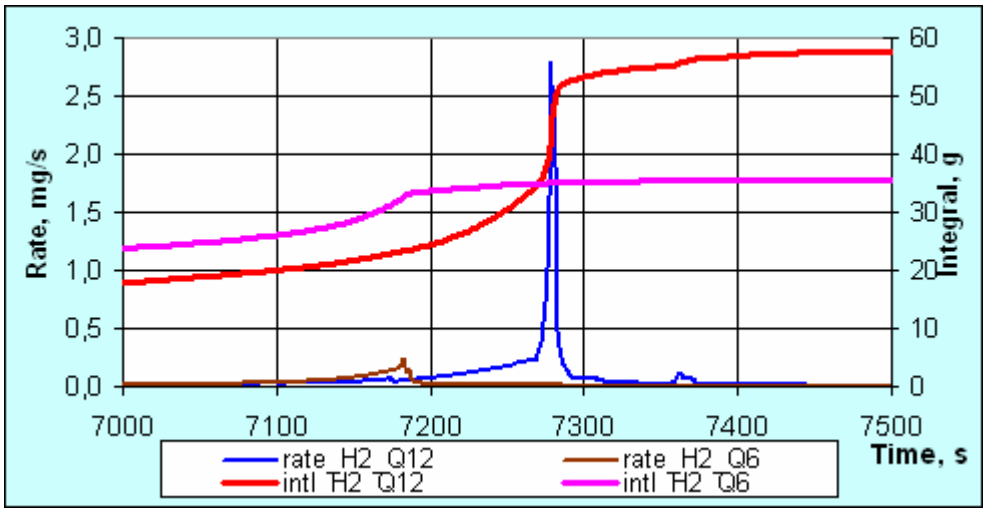

Figure 16: Comparison of hydrogen production for QUENCH-06 and QUENCH-12

The cracked oxide layer, which was intensively damaged on the surface of VVER claddings due to breakaway effect, has not more protective function and provides a high hydrogen penetration rate.

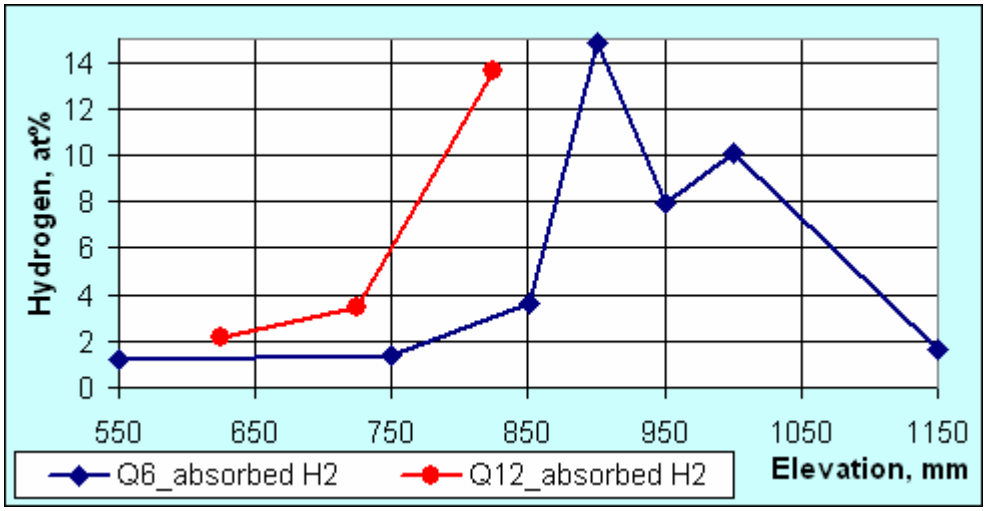

Figure 17: Comparison of hydrogen absorbed in claddings.

4 FUTURE PROGRAMME QUENCH-ACM

A new series "QUENCH-ACM" investigating test bundles with advanced cladding materials, i.e. M5, Duplex D4, ZIRLO, has been defined to be tested at elevated temperatures with subsequent quenching.

Besides the precursor VVER-type experiment QUENCH-12 which was already conducted in 2006, the QUENCH-ACM test series comprises three experiments, i.e. QUENCH-14 through 16 (see Tab. 3).

The test bundle arrangement for experiments QUENCH-14 (M5) and QUENCH-16 (Duplex) is identical to the standard one but different for QUENCH-15 (ZIRLO) due to a rod diameter of 9.5 mm and a pitch of 12.6 mm. The latter test bundle comprises 24 fuel rod simulators (heated rods), no unheated rod, and eight corner rods.

Cladding	Vendor	Reactor type	Dimen-sions, mm	Pitch, mm
M5	Areva	PWR	Ø 9.3 / 10.75	14.3
ZIRLO	Westinghouse	PWR	Ø 8.347 / 9. 5	12.6
Duplex Zry-4/D4	Areva	PWR	Ø 9.3 / 10.75	14.3
E110	Russia	VVER	Ø 7.73 / 9.13	12.75

Table 3: Cladding material and diameter of the fuel rod simulators and pitch for the QUENCH-ACM test series.

As in the Zry-4 experiments, fuel is represented by ZrO_2 pellets. The test section instrumentation will be as usual, i.e. thermocouples will be attached to the cladding, shroud, and cooling jacket at elevations between 50 mm and 1350 mm. The QUENCH-ACM test series is scheduled to be performed in the period of 2008-2010. Co-operations with respect to pre-test predictions and post-test calculations with severe accident codes, provision of material properties, and model development are welcome.

5 SUMMARY, CONCLUSIONS AND OUTLOOK

The isothermal and transient oxidation behaviour of the three advanced cladding materials DUPLEX, E110 and M5 in steam, oxygen and air were compared with the behaviour of the classical Zry-4. For all materials a parabolic time dependence of mass increase and oxide layer growth was found at least in the early phase. The oxidation rates depend on temperatures by Arrhenius functions. The activation energies differ for the different zirconium oxide crystal structures.

In the temperature range between 800 and 1000°C the breakaway effect was found for oxidation of E110 in steam and oxygen. At 1000°C the oxidation of Zry-4 shows this effect, too. The effect results in an enhanced oxidation. The time dependence changes from parabolic to nearly linear. For the D4 layer of the DUPLEX material and for M5 no breakaway takes place. The morphology of the spalled oxide layer parts differs significantly between E110 and Zry-4. They are much finer for E110 than for Zry-4. The intensive breakaway effect was also found for transient oxidation of E110 with heating rates below 0.1 K/s. For these low heating rates the time in which the materials are in the temperature range where the breakaway effect takes place is long enough for enhancing of oxidation. The strong influence of the breakaway effect on the severe accident behaviour of fuel rod bundles can be seen by comparison of the large scale bundle simulation tests QUENCH-6 and QUENCH-12. The hydrogen release of the QUENCH-12 bundle during reflooding, where massive spallation of oxidised parts takes place, was six times higher than of the QUENCH-6 bundle under comparable conditions.

Oxidation in air shows faster kinetics than in pure oxygen or steam. The reaction depends nearly linear on time. This is caused by the formation of a very porous oxide scale mixed with zirconium nitride which is formed at positions where (local) oxygen starvation occurs and sub-stoichiometric oxides are formed, i.g.at the oxide-metal phase boundary.

ACKNOWLEDGMENTS

The Zr1Nb (E110) and Zr2.5Nb (E125) material used in the VVER-type experiment QUENCH-12 for fuel rod simulators, grid spacers, and shroud was provided by Russian institutions in the context of the ISTC 1648.2 program. M5 and Duplex D4 rod claddings were delivered by AREVA. The ZIRLO cladding and pertinent grid spacer material was supplied by Westinghouse Electric Sweden AB.

The authors thank Ms. U. Stegmaier and Ms. P. Severloh for the metallographic investigations, Dr. R. Simon for the support in the XRA measurements of the tin distribution in the Duplex material. The author is also grateful to Dr. G. Schanz for the fruitful discussions.

REFERENCES

[1] L. Sepold, W. Hering, G. Schanz, W. Scholtyssek, M. Steinbrück, J. Stuckert: Nucl. Eng. & Design 237, 2157 (2007)

[2] J. Stuckert et al., “RESULTS OF THE QUENCH-12 REFLOOD EXPERIMENT WITH A VVER-TYPE BUNDLE,” 15th International Conference on Nuclear Engineering, Nagoya, Japan, April 22-26, 2007 (ICONE15-10257)

[3] L. Sepold, W. Hering, C. Homann, A. Miassoedov, G. Schanz, U. Stegmaier, M. Steinbrück, H. Steiner, J. Stuckert, "Experimental and Computational Results of the QUENCH-06 Test (OECD ISP-45)", FZKA 6664, Karlsruhe, February 2004

[4] G. Schanz, B Adroguer and A.Volchek: Nucl. Eng. & Design 232**,** 75 (2004)

[5] R. H. Zee, J. F. Watters and R. D. Davidson: Phys. Rev. B 34, 6895 (1986)

[6] M. Grosse, R. Simon: “Analysis of Tin Diffusion in Zircaloy-4 and Tin Redistribution after Steam Oxidation by means of X-ray Fluorescence Measurements”, to be published in Proceedings MSE 2008

[7] M. Steinbrück et al., “Prototypical Experiments on Air Oxidation of Zircaloy-4 at High Temperatures”, Transactions of the American Nuclear Society 94, 136 (2006)

[8] G. Schanz, M. Heck, Z. Hozer, L. Matus, I. Nagy, L. Sepold, U. Stegmaier, M. Steinbrück, H. Steiner, J. Stuckert, P. Windberg: “Results of the QUENCH-10 Experiment on Air Ingress“, Forschungszentrum Karlsruhe”, Report FZKA 7087, 2006

[9] M. Steinbrück, “OXIDATION OF ADVANCED ZIRCONIUM ALLOYS IN OXYGEN IN THE TEMPERATURE RANGE 600-1600 °C,” 16th International Conference on Nuclear Engineering, Orlando, FL, USA, May 11-15, 2008 (ICONE16-48054)

[10] M. Große, “COMPARISON OF THE HIGH TEMPERATURE OXIDATION BEHAVIOUR OF DIFFERENT CLADDING MATERIALS,” Proceedings of the Annual Meeting on Nuclear Technology, Karlsruhe, Germany, May 22-24, 2007

[11] J. Stuckert, A. Goryachev, M. Große, M. Heck, I. Ivanova, G. Schanz, L. Sepold, U. Stegmaier, M. Steinbrück: "Results of the QUENCH-12 Experiment on Reflood of a VVER-type Bundle", FZKA 7307, Karlsruhe, 2008

TOPSAFE
Dubrovnik, Croatia, 30.09 - 3.10.2008

AN EXAMPLE OF RISK INFORMED METHODOLOGIES FOR ACCIDENT ANALYSIS IN A FUEL FABRICATION PLANT: THE JUZBADO INTEGRATED SAFETY ANALYSIS PROJECT

Óscar Zurrón-Cifuentes, Carolina Álvaro-Pérez
ENUSA Industrias avanzadas
Juzbado Fuel Fabrication Plant
Ctra. Salamanca-Ledesma, km. 26
37115 JUZBADO, Salamanca, Spain
ozc@fab.enusa.es, cap@fab.enusa.es

ABSTRACT

Since 2004, and in response to a specific request of the Spanish Regulatory Authority (CSN), ENUSA is undertaking the Juzbado Plant's Integrated Safety Analysis (ISA) project. An ISA is a systematic examination of plant's processes, equipment, structures and personnel activities to ensure that all relevant hazards that could result in unacceptable consequences have been adequately evaluated and the appropriate protective measures have been identified. The relevant hazards considered are all those which can lead to radiological consequences, basically, nuclear criticality, contamination & irradiation, fire & explosion, chemical or environmental. The applied methodology foresees to split the plant into basic pieces of analysis (nodes) and carefully peer at each of them identifying hazards. This allows the identification of all credible accident scenarios which are then analyzed in order to asses the risk (high, intermediate or low) of their consequences. The set of appropriate safeguards is then identified, and from it, the so called Items Relied On For Safety (IROFS) are selected depending on the rank of risk of the accident scenario. These IROFS are those safeguards which ensure safety even in the case that the rest of safeguards have been lost. The project implies a number of different activities which must be performed by the plant staff at all the levels and with different skills and qualifications, which means to implement a specific organizational structure to manage the project and training of all the personnel involved. This paper shows the key ideas related to ISA implementation and the approach chosen to deal with it, along with the conclusions reached so far. ENUSA considers that this project will qualitatively increase the degree of knowledge of the potential initiating events, which will lead to an optimization of the safety management of the plant.

1 INTRODUCTION

In 2004 and following a request of the Spanish Regulatory Authority (CSN), ENUSA started at the Juzbado LEU Fuel Fabrication Plant the development and implementation of a risk-informed methodology for accident analysis, which was called the Juzbado Plant Integrated Safety Analysis (ISA) project. By that time, ENUSA was involved in renewal of the Juzbado Plant Operating License and ISA was one of the items open to discussion with CSN. Several profitable meetings were held to clarify positions in issues such as regulatory basis, scope of the analysis, and time-schedule for the project before CSN issued in May 2004 the Official Request establishing the regulatory basis for the ISA and convening ENUSA to

submit a planning for the project. The decision was taken not to issue any specific Spanish regulation on ISA but instead refer to the US 10 CFR Part 70.

As established in the CSN's Official Request, an ISA is a systematic examination of a plant's processes, equipment, structures and personnel activities to ensure that all relevant hazards that could result in unacceptable consequences have been adequately evaluated and the appropriate protective measures have been identified. The relevant hazards considered are all those which can lead to radiological consequences, basically, nuclear criticality, contamination & irradiation, fire & explosion, chemical or environmental, along with natural phenomena (floods, quakes, hurricanes, etc.) and any other external event which could be safety related.

It took ENUSA almost one year to prepare the infrastructure needed to go through the project. Upon receipt of the Official Request, a functional organization was built-up. The first task of this organization was to identify a methodology which assured compliance with CSN's requirements while fitting as much as possible with the Juzbado Plant specific idiosyncrasy. In this context, and taking into account the fact that ISA was already under implementation in USA following NRC requirements, the decision was taken to contact GNF-Wilmington in order to ascertain whether its ISA methodology would be applicable to the Juzbado Plant. Indeed it was, so a team was sent to Wilmington in order to imbed the methodology, adapt it the Juzbado Plant and produce the action plan to comply with the CSN's request. The outcome of this process resulted in a number of different activities which must be performed by the plant staff at all the levels and with different skills and qualifications, which implied enhancement of the initial functional organization involving personnel from different areas in the plant. Thus a multi-disciplinary organizational structure was designed to manage the project and train all the personnel involved.

The following paragraphs show the key ideas related to ISA implementation and the approach chosen to deal with it, along with the conclusions reached so far.

2 ORGANIZATION & TRAINING

2.1 Organizational Setup

The functional organization which runs the project is shown in Figure 1. It consists of three levels: ISA teams, ISA experts and Project Manager (PM).

The primary level and real heart of the project are the ISA teams. These are constructed so that every single node (*i.e.* smallest piece of analysis) is analysed by a specific ISA team. Accordingly, team members are selected in such a way that they are able to bring to the group all the operational and technical experience necessary to conduct the job and in this sense, the participation of personnel directly related with shop-floor operations is absolutely essential. Thus, the teams are comprised, a least, by 2 ISA experts (personnel trained on the ISA methodology), 1 expert from each of the safety disciplines (that is, Nuclear Criticality, Health Physics & Industrial Safety), 1 plant engineer and 1 shop-floor operator. Of course, these teams can be complemented with members experienced on the node subject to analysis, including maintenance persons.

ISA experts are intended to coordinate the team meetings, lead the discussions of the group and document the whole process. They are specifically trained on the ISA methodology and in particular, on the hazard analysis techniques being applied. ISA experts are qualified according to internal procedures. The decision was taken to include 2 ISA experts in each team, so that one of them could lead the meetings, focusing mainly on the discussions, whilst the other could take care of the administrative tasks of the process.

The project is coordinated by a PM to whom the ISA experts in charge of the different teams report.

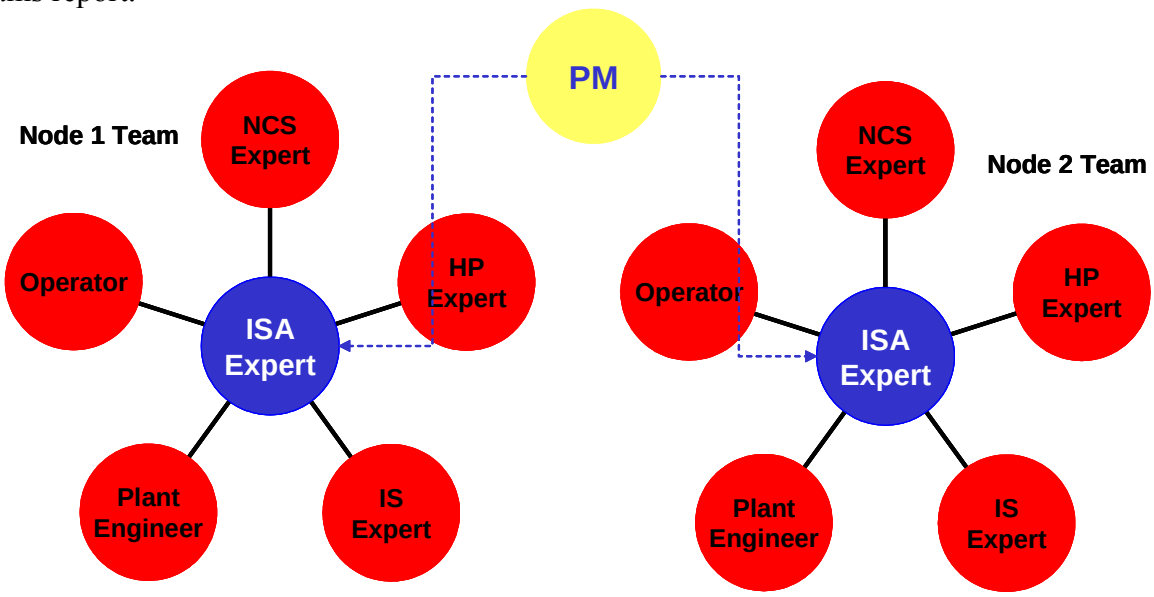

Figure 1: ISA Organizational Setup

2.2 Training activities

The training program for the personnel involved in the ISA Project has been designed on a "cascade" basis, so that it started involving a small group of persons who would deliver the knowledge downstream when required.

Thus, by the end of 2004 the selected personnel was subjected to a comprehensive training course devoted to hazard analysis methodologies at the Juzbado Plant's premises, which was addressed, basically, to engineers and safety people intended to later become ISA experts. This group constituted the seed of the actual functional organization.

The training at the PM level was complemented with a 1-week specific visit to GNF-Wilmington held by the end of January 2005. This visit allowed developing the ENUSA's ISA approach to be later applied. Once this task was completed, the final training of the ISA experts was conducted by early May 2005 with a 3-day course held at the Juzbado premises, to which CSN staff members were invited to attend. After this six-month period, the initial organization was ready to begin the job.

Training at ISA team level (if needed) is foreseen after selection of the members and in any case, prior to the first meeting of each group. In this training, team members are subjected to an ISA methodology induction along with the specificities of the hazard analysis technique chosen for the node under consideration.

By mid-May 2005 and upon completion of the initial training program, the ENUSA's ISA procedure and planning was submitted to the CSN fulfilling the requirement of the Regulator's Official Request.

3 RISK ASSESSMENT

Figure 2 shows the front end of the chosen approach for the Juzbado Plant's Integrated Safety Analysis. The first step was to split the Plant into areas of analysis following process or functional criteria and then, split the areas into nodes, which are the smallest piece to look

upon and thus, the basic unit for the study. 20 areas and 117 nodes were identified in a first approximation, though it is likely that these numbers change as the project evolves.

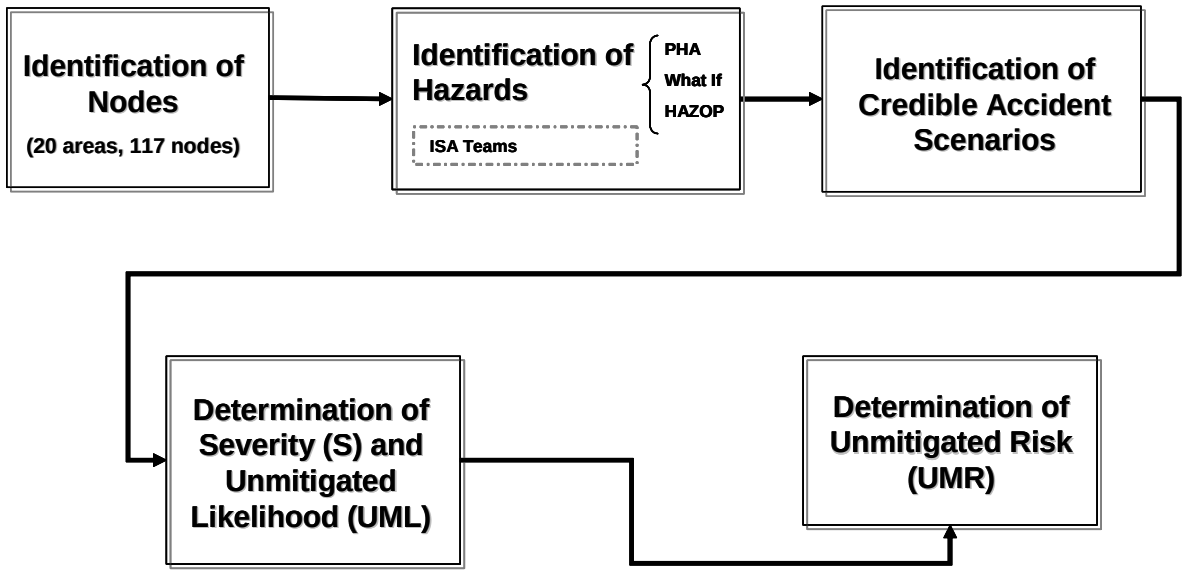

Figure 2**:** ENUSA's ISA Approach (I)

The ISA team for the specific node is then selected and trained (when necessary). The work begins with the identification of hazards, which is done by means of methods as *What if* or HAZOP (for more complex nodes). This allows the identification of all credible accident scenarios and for each of which, evaluating all possible causes and consequences. At this stage, it is important to highlight that the idea is to identify all the consequences, no matter whether they are radiological or not. Once every individual consequence is identified, the Severity and Unmitigated Likelihood (UML) of the sequence are assessed and combined to derive the Unmitigated Risk (UMR) associated with the considered accident scenario.

3.1 Severity

The severity matrix adopted by ENUSA is shown in Table 1. This matrix is based upon the criteria established in Appendix A of NUREG-1520 [1]. The first two columns of Table 1 refer to Nuclear Criticality Safety (NCS) related events which are not included in reference [1] but that have been considered for completeness. Therefore, NCS events are categorised in terms of the remaining number of Independent Control Parameters (ICP) which remain in place after the initiator so that the rank will depend on whether there are Multiple Parameters being controlled (MCP) or just a Single Parameter with several controls (OCP).

Regarding purely radiological-related events, the figures included in Table 1 slightly differ from those included in reference [1]. In this case, the rational behind the figures was to conservatively accommodate their values to the current Spanish regulations on Radiological Protection. Furthermore, the severity of events related to effluent discharges has been related to the Juzbado Plant's operational license and notification limits.

Remarkably enough there is no reference to chemical doses in Table 1, as this is very low risk at the Juzbado Plant and any case with purely industrial safety related consequences, but not radiological. As all the consequences are recorded in the ISA, the decision was taken to rank as level 1 all the events that could result in conventional (non-radiological) damage to the workers, although they fall out of the severity matrix.

Table 1: Severity Matrix

Rank	Criticality		Radiological	
	MCP	**OCP**	**Workers**	**Public**
3	Lost of all ICP	Lost of all controls	D > 1Sv	D > 250mSv
				Ingestion of more than 30mg of U
				Effluent release above License limits
2	Lost of one or several ICP such as only **ONE** ICP remains intact	Lost of one or several controls such us only **ONE** control remains intact	50mSv ≤ D ≤ 1Sv	5mSv ≤ D ≤ 250mSv
				Effluent release above Notification limits
1	Lost of any ICP such as the Double Contingency Principle remains intact	Lost of any control such as the Double Contingency Principle remains intact	D < 50mSv	D < 5mSv
				Effluent release below Notification limits

3.2 Unmitigated Likelihood

Table 2 shows the Unmitigated Likelihood table applied by ENUSA. It is important to note that this is an unmitigated value and thus, stands for the likelihood of the accident sequence without taking into account the specific safeguards already implemented (or to implement). A 50 year Plant lifetime was assumed to distinguish between credible and incredible sequences. On the other hand, a term of 2 years was considered as a reasonable value to rank the UML of credible sequences.

Table 2: Unmitigated Likelihood

Rank	Frequency	Likelihood
3	More frequent than once every 2 years	Likely to occur in the immediate future
2	Every 2 to 50 years	Likely to occur during the plant lifetime
1	Less than once every 50 years	Unlikely to occur during the plant lifetime
0	Incredible	Non-distinguishable from zero

3.3 Unmitigated Risk

The combination of the previously assessed values for Severity and UML leads to the Unmitigated Risk, as shown in Table 3. This matrix is more conservative that the one included in reference [1], which ranks as acceptable all risks below index 6. We consider as non-acceptable the intermediate risk scenarios, with risk index values of 3 and 4.

Table 3: Unmitigated Risk

	UML			
S	**0**	**1**	**2**	**3**
3	**Null**	**Intermediate**	**High**	**High**
2	**Null**	**Low**	**Intermediate**	**High**
1	**Null**	**Low**	**Low**	**Low**

As we soon see, this risk assignment is used by the ISA team to assess the appropriate level of assurance for the safeguards.

4 SAFEGUARDS, IROFS AND OVERALL LIKELIHOOD

The back end of the process is shown in Figure 3. All the safeguards already implemented (or to implement) to either prevent or mitigate the effects of every single accident scenario are identified by the team members, including those related to low risk events.

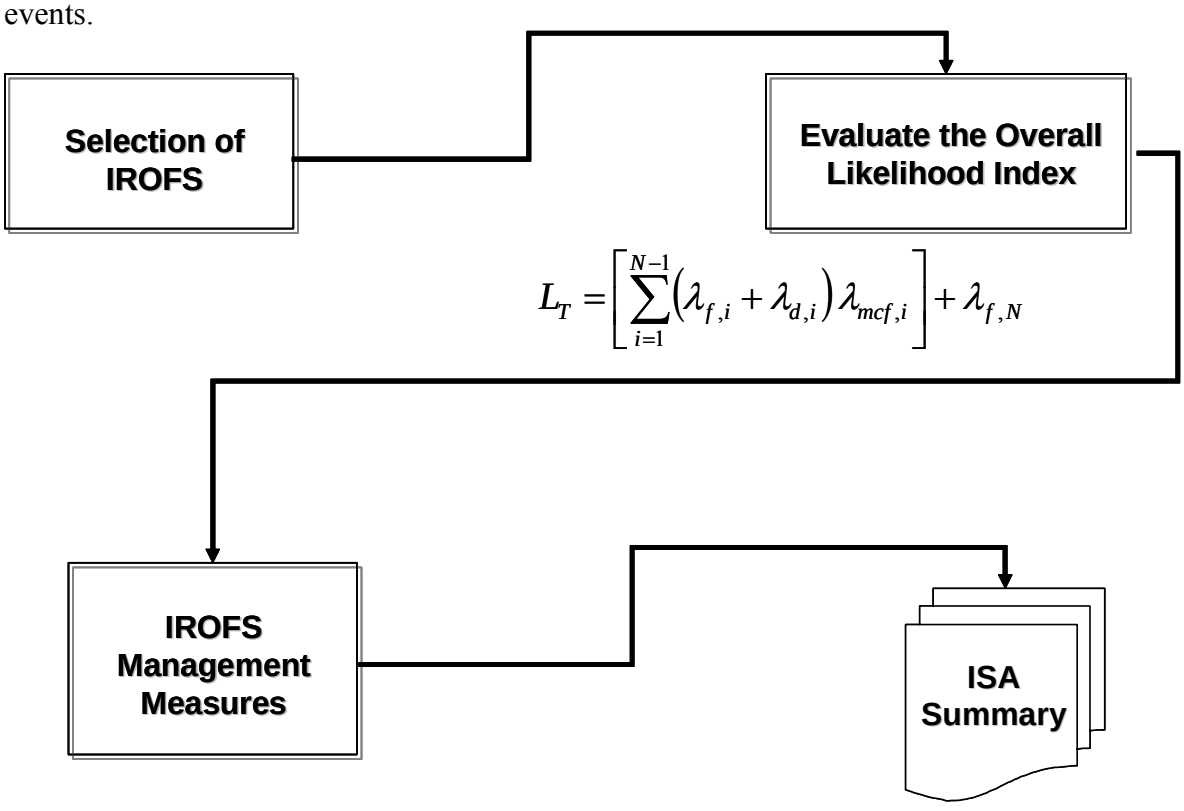

Figure 3**:** ENUSA's ISA Approach (and II)

Then, from this set of safeguards, the *Items Relied On For Safety* are selected for those intermediate and high risk accident scenarios. The IROFS are those safeguards which ensure safety even in the case that the rest of safeguards have been lost. At least two independent IROFS are identified for every intermediate and high level risk accident scenario. IROFS can

be either passive or active engineered controls, or enhanced administrative controls, but not purely administrative controls.

4.1 Overall Likelihood

Once the set of IROFS applicable to a specific scenario has been identified, the Overall Likelihood (L_T) index is computed. This takes into account the individual IROFS failure's frequency, the time period (duration) of IROFS failed condition prior to detection, and the existence of (other) independent IROFS.

Let us assume that N IROFS have been identified for mitigating a given sequence. The L_T index is then calculated by means of Eq. (1) below, derived following the criteria established in reference [2]:

$$L_T = \left[\sum_{i=1}^{N-1} \left(\lambda_{f,i} + \lambda_{d,i} \right) \lambda_{mcf,i} \right] + \lambda_{f,N} \quad (1)$$

Where,

$\lambda_{f,i}$ is the frequency index of failure per year of IROFS ith; $\lambda_{d,i}$ is the failure duration index of IROFS ith; and $\lambda_{mcf,i}$ is the common mode failure factor of IROFS ith. Both $\lambda_{f,i}$ and $\lambda_{d,i}$ are calculated by taking Log_{10} to the appropriate values of frequency and duration of failure as tabulated in the existing industry data bases, whereas $\lambda_{mcf,i}$ can either equal to 1 if IROFS ith is completely independent from all other IROFS being considered, or to 0 providing IROFS ith is subject to common mode failure with any other IROFS. Finally, $\lambda_{f,N}$ represents the frequency index of failure for the last IROFS in the string. Conservatively, it is assumed that this last IROFS is always that with the smallest duration index.

The so computed L_T index is then compared with the acceptance criteria shown in Table 4. L_T index must always be smaller than the corresponding clearance criteria. Should L_T index fall out of the limits, the IROFS selection is considered no longer valid and then, a new set of IROFS must be selected and newly subjected to the acceptance process.

Table 4: L_T index acceptance criteria

L_T	Likelihood per year	Comments
-6	1.00E-06	
-5	1.00E-05	
-4	1.00E-04	Acceptable limit for High Consequence sequences
-3	1.00E-03	Acceptable limit for Intermediate Consequence sequences
-2	1.00E-02	
-1	1.00E-01	

Once IROFS is validated according to the above described acceptance criteria, a specific management program is implemented according to established procedures. The scope of the program depends on the type of IROFS (passive or active, engineered or administrative,

etc.) and their importance (level of UMR they protect against to). This program is intended to ensure the reliability and availability of IROFS to perform its function at any time.

5 ISA SUMMARIES

All the above described process is recorded and documented using software specifically developed for process hazard analysis applications (Hazard Review LEADER™). The software allows maintaining a data base with the information generated by the ISA team meetings and drafting reports to document the process.

These reports are then reviewed by the ISA experts who leaded the meetings and subjected to management approval. Once all the nodes belonging to an area have been analyzed and documented, an ISA summary for the corresponding area is to be issued and submitted to CSN for approval.

6 FINAL REMARKS

The initial planning submitted to CSN on 2005 foresaw a minimum of 5 years for the whole project to be finalised. After almost 3 years of work, 51 nodes have been analysed with about 1000 accident sequences being identified, out of which 33 where ranked as intermediate risk, none as high risk.

The decision was taken to implement a design modification in the equipment to get rid of one of those sequences and thus, to avoid the implementation of IROFS. Therefore, 32 sets of IROFS have been identified up to the time this paper was written. In most cases, IROFS were selected from the safeguards currently available, but some of them have led to design modifications in the Plant to comply with the ISA requirements for IROFS.

Although the project is still ongoing, ENUSA considers that the implementation of the ISA program is increasing qualitatively the degree of knowledge of the potential initiating events and then, leading to an optimization of the safety management of the plant.

ACKNOWLEDGMENTS

The authors gratefully acknowledge the work done by all the ENUSA staff involved in the ISA project for the last 3 years. Also, we would like to thank the help of the GNF-Wilmington's ISA team during these years and in particular, the work done by James W. Reeves.

REFERENCES

[1] Standard Review Plan for the Review of a License Application for a Fuel Cycle Facility, Appendix A. NUREG-1520. US NRC (2002).

[2] Layer of Protection Analysis. Centre for Chemical Process Safety, New York (2001).

TOPSAFE
Dubrovnik, Croatia, 30.09 - 3.10.2008

Safety Improvements on Fuel Rod Behavior Because of Axial Fission Gas Transport Modeling

M.T. del Barrio, L.E. Herranz
Unit of Nuclear Safety Research, CIEMAT
Avenida Complutense 22, 28040 Madrid, Spain
mt.barrio@ciemat.es, luisen.herranz @ciemat.es

ABSTRACT

Fission gas release (FGR) to the gap during irradiation is not uniform along the fuel rod length. The axial profiles of temperature and neutron flux cause higher releases at high temperature and high power regions. Such lack of uniformity could be even enhanced in transients where FGR at specific regions are fostered. The importance of these scenarios lies in the analytical approach adopted by most present fuel performance codes, where axial gradients are neglected and transport processes are assumed to occur just along the radial direction.

This paper investigates the major features of axial transport of fission gases and critically assesses the potential impact on fuel rod behaviour. Experimental evidences are gathered and bases of existing models are reviewed. Estimates of characteristic transport times in postulated scenarios are presented.

According to this study, consideration of the axial fission gas transport in fuel performance codes might be necessary at the beginning of irradiation, as the gap is still open and the in-gap gas content has not been extensively contaminated by Xenon (Xe) and Krypton (Kr). Both gases degrade the thermal properties of the gas mixture with respect to Helium (He) ones and, as a consequence of the thermal feedback of FGR, release is even further enhanced at those regions with higher Xe and Kr content. Hence, the present assumption of instantaneous gas mixture in the fuel rod gap might not be conservative.

The models proposed in the literature can be grouped in two categories: diffusion models and diffusion-convection models. The latter offers the most comprehensive description; however, some of them may be regarded as too complex to be implemented in present fuel performance codes.

1 INTRODUCTION

The fission gases released from the fuel get mixed with the gases in the gap. This mixing transient takes time depending on specific conditions of the fuel rod and FGR. Anyhow, mixing time is bounded between two asymptotic situations: instantaneous mixing and fully segregated emission (i.e., released gases push away the pre-existing gas mixture at the given location). The former involves a much lighter modification of the gap thermal conductivity than the latter (Xe and Kr thermal conductivities are roughly 20 times lower than He one), because of which the feedback on FGR can be significant.

Experimental evidences show that as the gases are released from the pellet, there is an initially local accumulation. Then gases start dilution in the existing gas mixture with a finite kinetics driven by the local concentration and pressure spikes, so that gases are transported

due to concentration and pressure gradients until reaching an equilibrium situation in the rod. As a consequence, the temperature evolution at the location where FGR occurs can be described as in Figure 1.

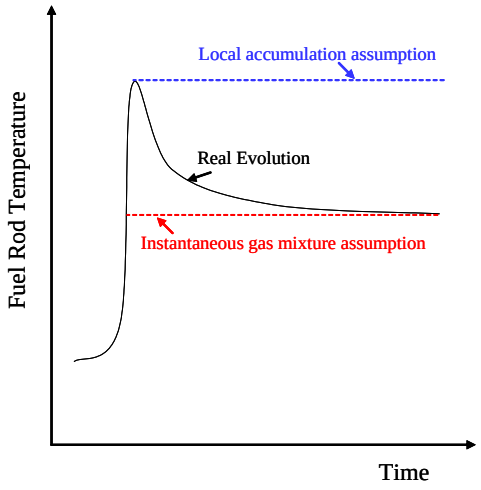

Figure 1**:** Comparison of different gas transport assumptions on fuel thermal behaviour.

Despite experimental evidences of the outlined dilution kinetics, most of the fuel rod performance codes do not consider any axial transport phenomenon, so that this mixing transient is not accounted for. Instead, they assume a non-conservative instantaneous mixing. Namely, fuel temperature at the release location is underestimated with respect to the real situation and, given the Temperature-FGR feedback, FGR as well.

Overall, the transport scenario is drastically affected by fuel and, more specifically, by the closure status of gap. As long as the gap is open, there will be a perfect axial communication in the gap all along the fuel stack. Under these conditions, the gas transport mechanisms inside the fuel rod do have a diffusive nature (i.e., axial concentration gradient) and a convective one (i.e., axial pressure gradient). However, as the gap becomes closed the transport is severely hindered. In addition, the higher the burnup the higher contamination of the rod filling gas by Xe and Kr and, as a result, the effect of any additional FGR becomes less significant progressively. Moreover, gap thermal resistance relevance in the global heat transfer turns out less significant as its thermal resistance decreases due to gap shrinkage.

2 STATE OF THE ART

The theoretical approaches of axial gas transport can be grouped in: diffusive models [1, 2] and diffusive-convective models [3, 4 and 5]. Coupling of diffusion and convection processes makes the latter group rather more complex. In order to overcome such complexity, Nakajima [5] assumes that convection is much faster than diffusion, so that he imposes an instantaneous convective transport, diffusion starting once pressure has been equalized along the fuel rod. This simplicity turns Nakajima's model into a good alternative to be implemented into fuel performance codes. All the models neglect radial transport of the gas.

Some of the models consider the main fission gas release (Xe and Kr), while others just take conservatively into account Xe as the fission gas species (its fission yield being higher and lower diffusion velocity than Kr ones). Moreover, the models just consider diffusion between binary species, He-Xe or He-Kr, i.e., between one of the fission gas and the initial filling gas, but never between fission gases or in ternary diffusive processes.

2.1 Gas Transport Model [5]

The transport model proposed by Nakajima [5] has been reviewed and their equations developed and implemented in a FORTRAN stand-alone code. The model considers two gas species (He and Xe) and splits the fuel rod in several axial nodes (up to twelve), which may have different void volumes and temperatures (within each node gases distribute uniformly).

2.1.1 Convective transport

The convective flow due to pressure gradient causes a macroscopic gas flow toward rod plenum. Such flow is considered much faster than FGR and interdiffusion phenomena, so that instantaneous gas flow and pressure equalization are assumed.

The total amount of gas moles in each axial node:

$$n_j = \sum_x n_{x,j} \qquad (x=He, Xe) \tag{1}$$

And the total gas moles in the rod:

$$n = \sum_j n_j \tag{2}$$

So, the rod internal pressure after a FGR spike can be estimated by means of the ideal gas law:

$$P = nR \frac{1}{\sum_j (V/T)_j} \tag{3}$$

Hence, the amount of gases in each axial node after pressure equalization is given by:

$$n'_j = \frac{P}{R}\left(\frac{V}{T}\right)_j \tag{4}$$

The difference n_j and n'_j, Δn_j, corresponds to the number of gas moles before and after pressure equalization. The pressure gradient induced by the xenon release will promote the convective transport to the upper and lower axial nodes. At the location of the release, j_{FGR}, before any convective transport, the amount of gas in such node corresponds to adding the gas moles released ($n_{FGR,j_{FGR}}$) to the previous gas content ($n^b_{Xe,j_{FGR}} + n^b_{He,j_{FGR}}$):

$$n_{j_{FGR}} = n^b_{Xe,j_{FGR}} + n^b_{He,j_{FGR}} + n_{FGR,j_{FGR}} \tag{5}$$

Then, the gas fractions at the release node are updated as:

$$f_{He,j_{FGR}} = \frac{n_{He,j_{FGR}}}{n_{He,j_{FGR}} + n_{Xe,j_{FGR}}} = \frac{f^{b}_{He,j_{FGR}} \cdot n^{b}_{j_{FGR}}}{n_{He,j_{FGR}} + n_{Xe,j_{FGR}}} \quad (6)$$

$$f_{Xe,j_{FGR}} = \frac{n_{Xe,j_{FGR}}}{n_{He,j_{FGR}} + n_{Xe,j_{FGR}}} = \frac{f^{b}_{Xe,j_{FGR}} \cdot n^{b}_{j_{FGR}} + n_{FGR,j_{FGR}}}{n_{He,j_{FGR}} + n_{Xe,j_{FGR}}} \quad (7)$$

Estimate of the convective mole transport from the FGR node to upward and downward adjacent nodes proceeds in a stepwise fashion. It means that from release node, the gas exceeding the $n'_{j_{FGR}}$ will be pushed up and down to the adjacent nodes according to:

$$n_{j_{FGR} \to j+1} = \sum_{i=j+1}^{plenum} \Delta n_i \quad (8)$$

$$n_{j_{FGR} \to j-1} = \sum_{i=j-1}^{1} \Delta n_i \quad (9)$$

Once the gas lumps move to the upper and lower nodes, they are mixed with the gases inside the node. Therefore, these receiving nodes turn into the new source nodes. The gas fraction will change accordingly to the amount and fraction of gases transferred and the previous gases in the axial node:

$$f_{Xe,j+1} = \frac{n_{Xe,j+1}}{n_{He,j+1} + n_{Xe,j+1}} = \frac{f^{b}_{Xe,j+1} \cdot n^{b}_{j+1} + f_{Xe,j_{FGR}} \cdot n_{j_{FGR} \to j+1}}{f^{b}_{He,j+1} \cdot n^{b}_{j+1} + f_{He,j_{FGR}} \cdot n_{j_{FGR} \to j+1} + f^{b}_{Xe,j+1} \cdot n^{b}_{j+1} + f_{Xe,j_{FGR}} \cdot n_{j_{FGR} \to j+1}} \quad (10)$$

$$f_{Xe,j-1} = \frac{n_{Xe,j-1}}{n_{He,j-1} + n_{Xe,j-1}} = \frac{f^{b}_{Xe,j-1} \cdot n^{b}_{j-1} + f_{Xe,j_{FGR}} \cdot n_{j_{FGR} \to j-1}}{f^{b}_{He,j-1} \cdot n^{b}_{j-1} + f_{He,j_{FGR}} \cdot n_{j_{FGR} \to j-1} + f^{b}_{Xe,j-1} \cdot n^{b}_{j-1} + f_{Xe,j_{FGR}} \cdot n_{j_{FGR} \to j-1}} \quad (11)$$

The transport scheme, described above between FGR node and j+1 and j-1, is repeated in j+1 and j-1 in the upward and downward direction, respectively, up to achieve the plenum or the first (bottom) axial node.

2.1.2 Diffusive transport

Once the gas moles are distributed by instantaneous convective flux the diffusive transport starts governed by the gas concentration gradient between adjacent nodes. The diffusion equation is formulated by means of the Fick's first law. The molar gas flux, G_x, of the x gas species from j to j+1 is given by:

$$G_x\left(j \to j+1\right) = F_{j,j+1}\left[\left(C_{x,j} - C_{x,j+1}\right) - \left(\overline{C}_{x,j} - \overline{C}_{x,j+1}\right)\right] \quad (12)$$

Where the first term corresponds to the Fick's first law, whereas the second is a correction for the temperature difference between axial nodes ($C_{x,j} \neq C_{x,j+1}$). The molar gas flux equation is integrated in periods of 1 second. Anyhow, the variables involved in Eq.(12) are calculated through the following expressions:

$$F_{j,j+1} = \frac{A_j D_{He-Xe,j} A_{j+1} D_{He-Xe,j+1}}{A_{j+1} D_{He-Xe,j+1} \Delta z_j + A_j D_{He-Xe,j} \Delta z_{j+1}} \quad (13)$$

$C_{x,j}$ = concentration of gas species x in axial node j

$$\overline{C}_{x,j} = \frac{P \cdot \left(f_{i,j} + f_{i,j+1}\right)}{RT_j} \quad (14)$$

$$\overline{C}_{x,j+1} = \frac{P \cdot \left(f_{i,j} + f_{i,j+1}\right)}{RT_{j+1}} \quad (15)$$

Δz_j = axial length of segment

$D_{He-Xe,j}$ = diffusion constant (m^2/s) of He-Xe mixture in axial node j

$$D_{He-Xe,j} = \frac{3}{8}\left(\frac{\pi RT_j}{2M^*}\right)^{1/2} \frac{RT_j}{P\pi\left(d_{He-Xe}\right)^2} \quad (16)$$

where

$$M^* = \frac{m_{He} \cdot m_{Xe}}{m_{He} + m_{Xe}} \quad (17)$$

m_i = molecular weight of species i

$d_{He-Xe} = \frac{1}{2}\left(d_{He} + d_{Xe}\right)$ = atomic diameter average of gas species

The diffusion constant is fitted with a d_{He-Xe} value of $3.45 \cdot 10^{-10}$ m to fit with the value of D_{He-Xe} experimentally observed of $3.58 \cdot 10^{-5}$ m^2/s at 0^oC and 1 atm [5].

3 SENSITIVITY ANALYSIS

In order to explore the gas transport sensitivity to parameters such as fuel length, initial rod pressure and FGR location, a set of calculations have been carried out. The scenario simulated is a fuel rod with characteristic pellet and clad dimensions of a commercial rod, a linear power rate of 10 kW/m and cooled by water at 240 ºC and 3.4 bar. The release is supposed to occur just in one node (out of a total of 9) at the beginning of the analysis.

3.1 Effect of the Rod Length

Short rods used in experimental reactors may behave differently from commercial ones. Two studies have been performed. The former simulates a fuel rod 0.36 m high with a plenum volume of $3.0 \cdot 10^{-6}$ m^3 and a cold radial gap of 50 μm. The latter is a similar rod, but the length is 10 times longer, 3.6 m, and the plenum volume is increased up to $20 \cdot 10^{-6}$ m^3. In the two cases, a Xe/(Xe+He) mole fraction of 58% was imposed in the middle axial node at the beginning of the analysis in a rod initially pressurized to 1 bar.

Figure 2 shows the normalized (i.e., initial Xe concentration at t=0 s is assumed to be 1.0) evolution of the Xe fraction at the release node in both rods. As expected, the mixing transient is faster in the short rod and the equilibrium is attained in a rather shorter period. This is consistent with the asymptotic solution of the Fick's law for a continuous FGR with zero Xe concentration at an infinite distance [6]. Under these boundary conditions, the time at which fission gas concentration at the plenum reaches 50% of the concentration at the release node, $\tau_{1/2}$, (assumed to be constant along time) can be approximated by:

$$\tau_{1/2} \approx \frac{z^2}{D} \tag{18}$$

Eq. (18) yields 0.72 h for the short rod and around 72 h for the long one.

These findings emphasize that extrapolation of the fast axial mixing observed in experimental fuel rods after a FGR spike is far away to be straight and it should be considered with utmost caution.

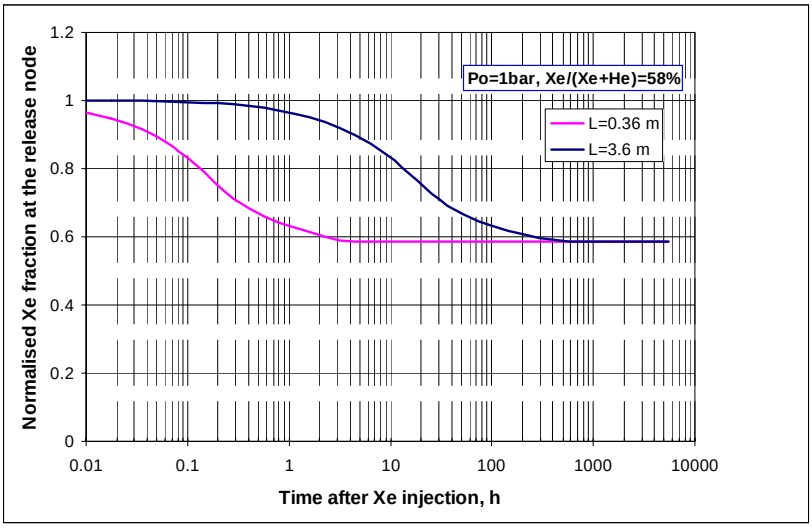

Figure 2**:** Effect of fuel rod length on fission gas transport

3.2 Effect of the Initial Rod Pressure

Two new simulations with an initial pressure of 25 bar have been conducted and compared to those presented above. As noted, an increase of the initial pressure results in longer mixing transients (consequently with the effect of pressure on gas diffusivities) in both rod lengths. Even further, the response time of short rods is notably shorter than for the long ones. An indirect measure of the potential effect of FGR spikes is the final equilibrium fraction, given the substantial weight of the initial He content in the total gas amount in the gap at 25 bar the Xe equilibrium concentration is reduced to a 5%.

In short, the higher the initial rod pressures the longer the mixing transients, due to changed gas diffusivities, and the less the effect of any FGR spike, due to higher initial HE content.

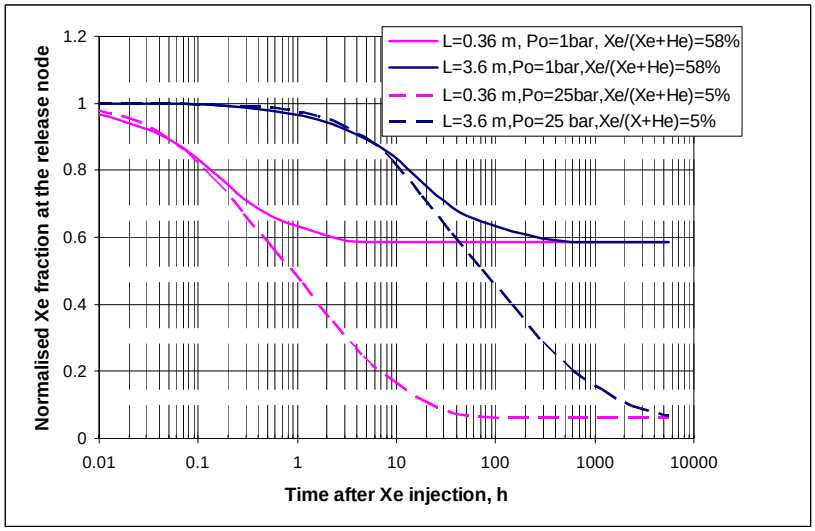

Figure 3**:** Effect of rod length in high and non-pressurized rods

Quantitatively speaking, an initial high pressure rod (i.e., 25 bar) would undergo mixing transients that, if similar to the one simulated, would be 10 times longer than at low pressure.

3.3 Effect of the release location

FGR during irradiation mainly takes place in the peak power zone. Experimentally [6], it has been observed that the longer the distance between releasing node and plenum the slower fission gases dilution. Such behaviour is attributed to the milder gradients set up. This is encapsulated in Eq. (18) where it can be noted that the diffusion time increases proportionally with the square of the diffusion distance.

Two new cases similar to the previous ones have been studied with the only difference being the FGR location, either at the top (node 8) or at the bottom (node 2) of the fuel stack. Consistently with previous discussion concerning diffusion times and gradient intensity (i.e., distance between concentration differences), Figure 4 shows that the higher the release location the shorter the time to reach equilibrium at the rod plenum. As shown in this example (high pressure, long rod), the delay resulting from a downward displacement of the FGR location can be n times the shorter diffusion time estimated, but within the same order of magnitude.

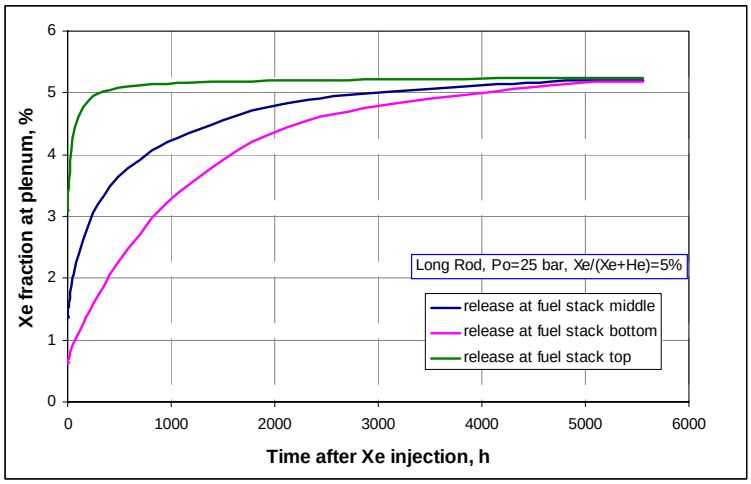

Figure 4**:** Effect of release location in a high pressurized rod

4 PROSPECTIVE INFLUENCE ON FUEL TEMPERATURE

A fission gas release is faster than the subsequent axial gas mixing and, particularly, a FGR spike, results in axial differences of gap thermal conductance. As a consequence, axial fuel temperature gradients would not be just a result of the power profile but also a consequence of the different gap thermal resistance at different rod locations. This scenario is away from most of codes that assume axial gas transport as an instantaneous phenomenon.

A prospective analysis of the potential influence of the gas transport on fuel temperature has been indirectly conducted. A PWR-UO2 fuel rod design has been simulated with FRAPCON-3 fuel rod performance code [7]. The main characteristics of the fuel rod at cold and under operating conditions are presented in Table 1.

Table 1: Main characteristic of simulated fuel rod

Item	Cold State	Hot State
Number of axial nodes	9(+1 for plenum)	
System pressure, bar	155.1	
Inlet coolant temperature, ^{o}C	292.4	
Fuel density, %TD	95.5	
U-235 enrichment, %	4.5	
Linear power, kW/m	10 (flat profile)	
Initial He moles	0.018719	
Active fuel rod, m	3.6576	3.6746
Cold free fuel rod volume, m^3	19.121E-06	16.236E-06
Cold plenum volume, m^3	9.5536E-06	8.8728E-06
Outer clad diameter, mm	9.5	9.50996
Inner clad diameter, mm	8.357	8.421
Cold Fuel-Clad Radial Gap, μm	82.5	68.6627
Cold Gap volume, m^3	9.5675E-06	7.3635E-06
Fuel pellet diameter, mm	4.096	4.1418
Initial He rod pressure, bar	23.5	59.86
Estimated Gap Temperature, K	--	629.8
Plenum Temperature, K	--	591.6

The effect of the Xe dilution kinetics has been approximated by a set of runs at different initial gap compositions. They have been taken from simulations with the model presented in previous sections, so that each gas concentration is associated to a specific time of a mixing transient. A low fuel power (10 kW/m) has been chosen to avoid any further FGR. The Xe injection was simulated to occur at the beginning of the analysis at the middle axial node. Detailed information concerning Xe injection is given in Table 2.

Table 2: Simulated Xe injection

Item	Value
Initial He moles	0.018719
Initial He rod pressure, bar	23.5
Cold Rod Pressure after Xe injection, bar	24.11
Xe injection at t=0, mol (at node 5)	4.8665E-04
Asymptotic Xe/(Xe+He)	2.53%

Figure 5 presents the estimated fuel centre temperature according to the gap fission gas composition evolution at the injection position. As can be observed, the assumption of an instantaneous mixing, results in a non-conservative temperature underestimate of about 100 ºC (greater than 10%) at the beginning of the transient and stays at those level for nearly 5 h. Given the link between fuel temperature and FGR, it can be foreseen that FGR will be fostered accordingly. This prospective study, however, cannot quantify this process. However, it has been shown that the temperature difference is high enough to recommend the axial mixing model implementation in fuel rod performance codes.

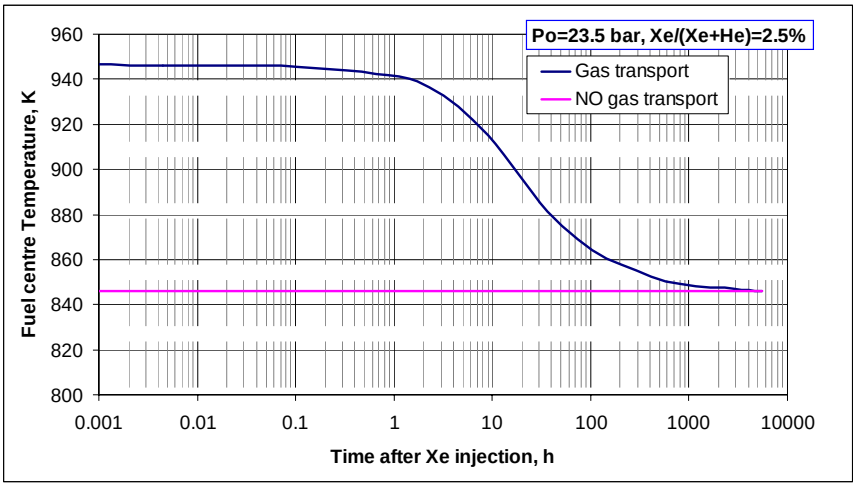

Figure 5**:** Fuel centre temperature evolution with and without gas transport model at the middle of the fuel stack

The estimated fuel centre temperature taking into account the axial gas transport is about 80-100 ^{o}C higher for more than 5 hours. This temperature difference is enough to promote further FGR at the gap and even increase the temperature difference. This further feedback can not be observed in this prospective approach since the axial gas transport model is not yet implemented in the fuel rod code. However, the fuel temperature difference and dilution times found are high enough to consider the implementation of an axial gas transport model in safety analysis.

5 CONCLUSIONS AND FINAL REMARKS

This paper analyzes the potential effects of a prompt FGR at a specific location of a fuel rod during reactor operation. Some of the main outcomes of this work can be summarized as follows:

- The time window of interest is bounded between a certain fuel irradiation that allows for a significant inter-granular fission gas accumulation and gap closure.
- The axial gas transport in pressurized commercial fuel rods happens to take longer than in non-pressurized experimental rods: Nonetheless, its effect is anticipated to be milder since under the same conditions the fraction of poisoning gases (i.e., Xe and Kr) is forcefully lower so that gap mixture properties would be closer to those of pure helium.
- The potential significance of not considering the axial gas transport during this effect can affect substantially the fuel rod behaviour during transients. By an indirect assessment based on using FRAPCON-3 under specific gap compositions, it has been

estimated that underestimations even higher than 10% could take place when the axial gas motion during transients is neglected. Such estimates are seen as approximate and, given the temperature-FGR feedback, significance is expected to be even more substantial.

- Modelling of axial convection and diffusion is complex and its implementation in current fuel performance codes are far from being straightforward. Nevertheless, by assuming that convection is an instantaneous process a remarkable simplification is gained. Presently, a stand-alone code has been built-up based on the concept proposed by Nakajima regarding instantaneous convection.

Further work foreseen is the implementation of the model into a fuel rod performance code such as FRAPCON-3.

ACKNOWLEDGMENTS

This work is framed within the CSN-CIEMAT agreement on “Thermo-Mechanical Behaviour of the Nuclear Fuel at High Burnup”.

REFERENCES

[1] J.C. KILLEEN and A. HAALAND, “Mixing of Argon and Helium in the Interior of a Fuel Rod,” HWR-186, OCDE Halden Reactor Project, Norway (1986)

[2] H. WALLIN and J. J. Serna, “Mixing of Fill Gas and Fission Gases in Fuel Rods,” HWR-360, OECD Halden Reactor Project, Norway (1994).

[3] M. KINOSHITA, “Axial Transport of Fission Gas in LWR Fuel Rods”. Proc. of the IAEA Specialist Meeting on Fuel Element Performance Computer Modelling, Preston, England (1982).

[4] M. NAKAMURA, K. Hiramoto and A. Maru, “Evaluation of LWR Fuel Rod Behaviour under Operational Transient Conditions,” Nuclear Engineering and Design 80, 49-63 (1984).

[5] T. NAKAJIMA, “FEMAXI-IV: A computer Code for the Analysis of Fuel Rod Behavior under Transient Conditions,” Nuclear Engineering and Design, 88, 69-84 (1985).

[6] C. VITANZA, T. Johnsen and J.M. Aasgaard, “Interdiffusion of Noble Gases. Results of an Experiment to Simulate Dilution of Fission Gases in a Fuel Rod,” HWR-295, OCDE Halden Reactor Project, Norway (1983)

[7] G. A. BERNA, C. E. Beyer, K. L. Davis and D. D. Lanning, “FRAPCON-3: A Computer Code for the Calculation of Steady-State, Thermal-Mechanical Behavior of Oxide Fuel Rods for High Burnup,” NUREG/CR-6534 Volume 2, Pacific Northwest National Laboratory, Richland, Washington, USA (1997)

AREVA-CERCA 10 years licence for fuel fabrication

Eric TORLINI – Thomas PIN

AREVA-CERCA
Les Berauds, B.P. 1114, 26104 Romans Cedex – France
Eric.torlini@areva.com, Thomas.pin@areva.com

ABSTRACT

Every ten years, each French Nuclear Installation (referred here after as INB for "Installation Nucléaire de Base") shall be subject to a safety evaluation review in order to obtain the operating licence for the next ten years period. The licence is delivered during a so called "Factory Permanent Group" review whose participants are a group of experts from the French Safety Authority (ASN), the French Institute for Radiation protection and Nuclear Safety (IRSN) and the User of the plant. The safety evaluation is conducted by both the User and the IRSN during at least a one year period before the Permanent Group review. During this period, the User shall demonstrate the conformity with regards to applicable standards of all the safety issues related to the factory operation such as criticality, radioprotection, seismicity, fire, external risks, etc…

After more than one year of study, CERCA factory in Romans (France) referred as INB # 63 has succeeded its safety evaluation review in late 2006 and is now licensed to operate safely till end of 2016.

The aim of this talk is to present the content of this project that has been conducted since end of 2005 and whose purpose is to ensure the sustainability of CERCA fuel fabrication factory in Romans (France), at least for the next ten years period.

1 PURPOSE

- Issue

Every ten years, each French Nuclear Installation shall be subject to a safety evaluation review in order to obtain the operating licence for the next ten years period.

As known, AREVA / CERCA is yearly manufacturing many types of Fuel Elements for Research Test Reactors & Material Test Reactors as well as thousands of molybdenum targets for the nuclear medical market. The factory is located in Romans (France) and is referred as INB 63 (Installation Nucléaire de Base # 63). The site is shared with FBFC as LWR plants type fuel factory through INB 98.

To operate, the INB 63 is subject to the authorization of the French Nuclear Safety Authority (ASN).

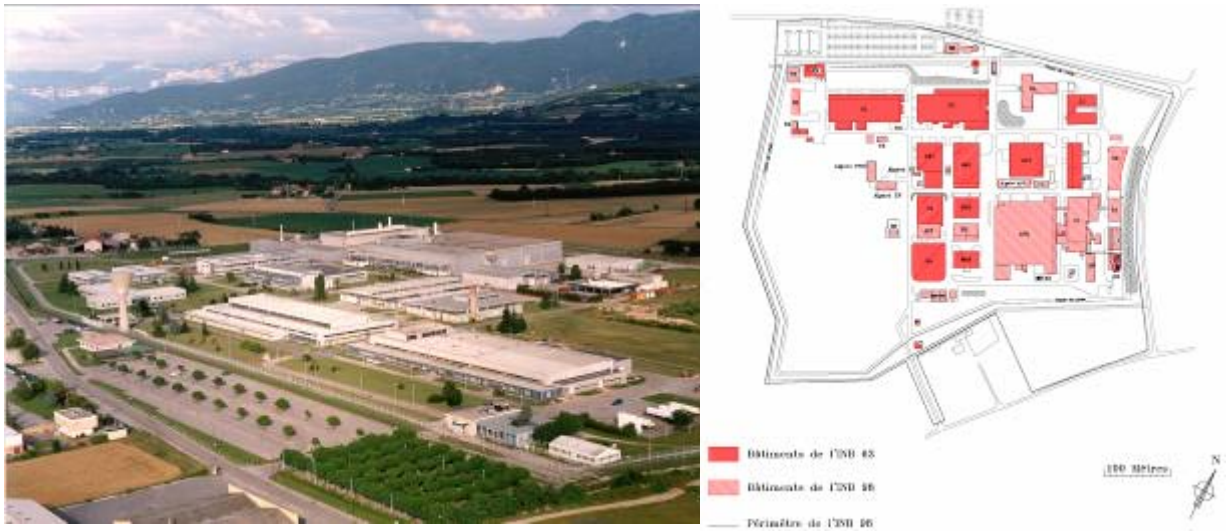

Picture and map of the CERCA / FBFC site

"ASN is tasked, on behalf of the State, with regulating nuclear safety and radiation protection in order to protect workers, patients, the public and the environment from the risks involved in nuclear activities. It also contributes to informing the citizens."

By end of 2006 and after a long preparatory period, CERCA was licensed by the ASN for ten years.

The purpose of this paper is to present the stakes of such an authorization and to highlight the main issues to address during the project.

- Be authorized

The authorization to run is subject to the prescriptions of the "Arrêté du 10 août 1984" (August 10th 1984 decree) related to the quality for the design, the construction and the operation of nuclear installations.

It is the responsibility of the operator to conform to the regulations. In front of the population, the ASN must guarantee the conformance of the Nuclear Installation (INB) operation to the decree.

CERCA no more authorized to run would deprive many research reactors of fuel and would significantly disrupt the production of molybdenum for medical exams. Therefore, be authorized is the challenge.

- Show the ability to operate safely

So, it is CERCAs everyday responsibility to maintain a high level of safety and security in its facilities. For this, a complete Safety, Security & Environment (SSE) system is deployed in order to ensure that all the practices conform to the safety regulations requirements.

- Be safe

The Nuclear Safety covers all the actions taken to prevent a nuclear accident or to limit its consequences.

Establishing and developing a strong safety organization is our priority for whole of our activities such as design, fabrication, storage & shipment of nuclear products.

Particularly, this organization must take into account all the equipment changes.

2 THE MAIN STEPS OF THE AUTHORIZATION PROCESS

➢ General project organization and planning

- French State side

The Nuclear Safety Authority is in charge of validating the authorization to run. This authorization may be delivered on the basis of a technical analysis which is conducted by the Institute for Radiation protection and Nuclear Safety.

"The IRSN is the expert in research and specialised assessments into nuclear and radiological risk serving public authorities". The IRSN is appointed by the Safety Authority.

During the safety evaluation period, the IRSN has constituted a project organization with a project manager and a team of experts on each discipline.

- AREVA / CERCA Side

CERCA has also constituted a project type organization in order to prepare whole of the documentation and to answer to the questions of the IRSN experts.

The team is lead by the Safety, Security and Environment Management department, and is also composed of personnel from the operation department of CERCA and from personnel from different engineering departments of AREVA.

Both teams always wanted to work closely in order to avoid any kind of misunderstanding. This spirit was a key factor of success.

The overall schedule of the project was as follow:

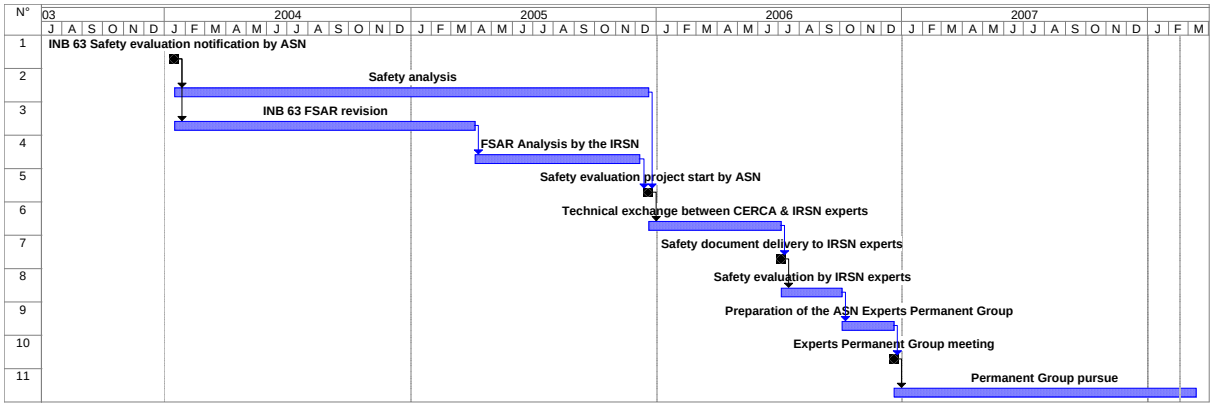

Overall schedule of the project

➢ Internal preparation period (Internal studies - FSAR revision)

The first step is to conduct internally a global safety analysis of the current situation in order to update the Final Safety Analysis Report (FSAR) and the Operating Guidelines. These documents must be an accurate picture of the factory at the beginning of the project in order to allow both parties to make their own diagnostic.

Doing the studies and updating the FSAR took about 1 ½ year. Obviously, the ideal would be to demonstrate safe people with safe processes on safe machines in a safe building. But the regulation always changes in a safer way and is more and more demanding. So, even if our level of safety is continuously upgraded, it remains still a little gap between what is required and what is in place.

The CERCA FSAR is divided in 3 volumes

- 1st volume : General description of the site and associated facilities
- 2nd volume : Detailed description and safety analysis of each workshop and facility
- 3rd volume : Global safety analysis

This structure allows anyone to easily access to the safety issues, either on the factory or at any work post.

The detailed evaluation review of each workshop and each process has permitted to show the strong points and the weak points of our way to operate. So it was easy to draw up an improvement program that could be submitted to the IRSN and implemented gradually.

Previously to the formal project start meeting, the revised FSAR as well as an improvement program proposal was transmitted to the IRSN.

➢ Project Start

The Safety evaluation review of the CERCA Nuclear installation is driven by the IRSN which scheduled a formal “project start meeting” that took place on Wednesday December 5th 2005 in Fontenay-aux-Roses (IRSN head office).

During this meeting, it was reminded the duties of each party, the way to work together and the main milestones:

- Project organization on both sides (IRSN & CERCA)
- IRSN experts assignments in CERCA
- Discussions
- Safety files delivery by CERCA to IRSN
- Safety evaluation by the IRSN experts
- Factory Permanent Group meeting preparation

➢ Evaluation by IRSN

This period took place between the project start and the safety files delivery to the IRSN by CERCA. It was a favourable period for technical exchanges between IRSN and AREVA/CERCA.

In ten months we had about 30 technical joint meetings.

As decided before, the relationship between the people was maintained very open in order to avoid any misunderstanding.

The following subjects were addressed:

- Criticality

Product sub-criticality follow-up during fabrication:

It is to demonstrate that, in any normal situation, the fabrication conditions allow to maintain Keff < 0,950 and in any accident situation, Keff < 0,975.

No accident occurrence in case of single failure:

Specific sketches have been elaborated in order to ensure that a double check is systematically done in case of a single criticality control mode

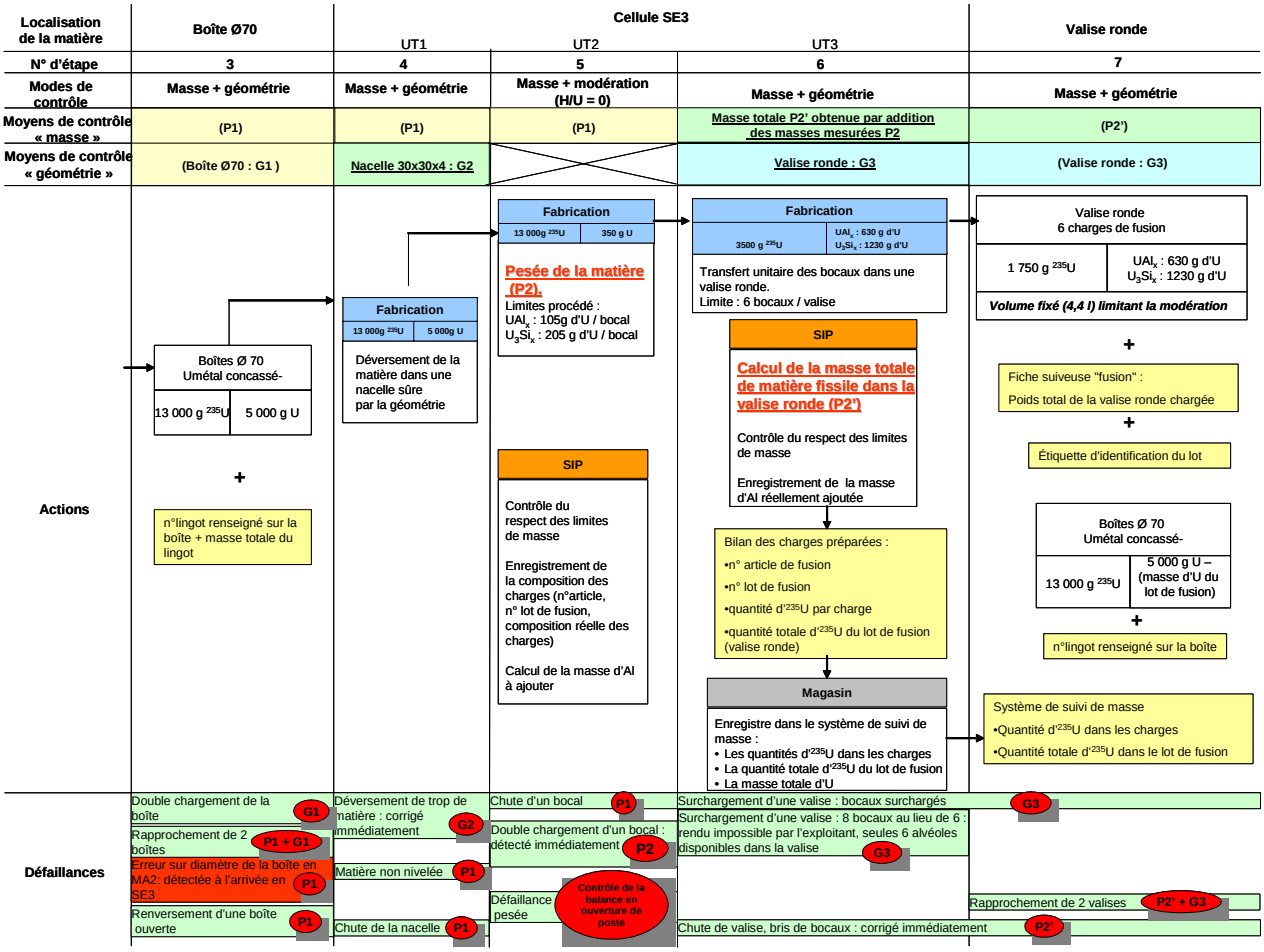

Example of specific sketch established to verify the presence of double check in case of single criticality control mode – case of a part of the uranium alloy elaboration process

- Human factor (Tokaï-Mura accident experience feedback)

  Consequences of high constraints on the safety during fabrication:

  The purpose of this study is to identify the risk of overstepping the red line by the operator in case of constraints in his work.

  An investigation program has been launched in order, first, to determine the sensitivity of CERCA to the human factor, second, to evaluate whether or not, specific measures should be taken. The methodology is based on an interview of the operators.

  Work post experience feedback evaluation

  Establishing the safety / criticality basic requirements & rules applicable to the work post

  Operator interviews

  Analysis

  Validation

  Action plan (if any)

  Current conclusions are that CERCA is quite sensitive to the human factor (indeed, there is one operator on each machine) and that the safety instructions are well understood and well observed.

- Radioprotection (internal exposure)

  In CERCA, the internal exposure of the operators is very low. Every handling of material is done under glove boxes or with the protection of a mask. Nevertheless, a few improvements are on going on some work posts organisation.

- Radiological cleanness / Material dissemination

  An evaluation was made on the safety of containments breaks during normal operation such as opening of a glove box airlock. A few minor improvements may be implemented.

- Seismicity

  The main seismicity issues were addressed during the previous evaluation review of the installation. A few equipments like storage compartments, tables, etc. remain to be fixed in order to fit with the current rules.

- Fire

  A complete fire risks evaluation has been conducted and ends up in a calorific load clearance which is on-going. Finally, the purpose of this study is to demonstrate that the local occurrence of a fire could not spread everywhere so as to set fire to a large part of the workshop.

- Equipment ageing

Each automated machine was analysed in order to identify if a loss or a defect of the control system could have consequences on the safety of the installation. The conclusions were that the safety is not sensitive to our automatisms.

- External risks (rain, snow, wind, storm, …)

  Series of risk evaluation have been requested by the IRSN to be conducted in the next 2 years. Those evaluations are on-going now.

- Aggression risks (gas explosion, truck explosion, plane crash, …)

  Same as above.

  A gas delivery cabinet will be moved away from the CERCA building in order to remove any accident due to a gas pipe breakdown.

- Hydrogeology

  A survey plan has been initiated in order to improve our capability to detect a potential contamination of the ground.

- Waste management

  This issue is managed at the site level. A global project is in charge of evacuating the wastes to the specialized sites of the ANDRA in conformance with the applicable rules.

  ANDRA is the National Radioactive Waste Management Agency. "ANDRA operates independently from the waste producers. …. It is responsible for the long term management of the waste produced in France."

  A selective sorting leads to direct the waste, either directly to the storage sites, or to the compacting facility of AREVA.

All those subjects were discussed with, and evaluated by the IRSN. Some of them where addressed during the preparation period of the Factory Permanent Group of Experts meeting. Some others require more time and so, a commitment from the INB 63.

The IRSN requested CERCA to produce nearly 20 safety analysis technical documents that were transmitted in due time. The IRSN was satisfied with the quality of those documents.

➢ <u>Preparation of the Factory Permanent Group</u>

It is the custom to organize a joint meeting between the IRSN and the operator in order to find acceptable solutions for the items that have not been agreed during the safety evaluation period.

This meeting is very important as it states on most of the issues.

The meeting took place on October 17th 2006. Its base of work was the IRSN report of INB 63 safety evaluation.

During the meeting, we confirmed the commitment of AREVA/CERCA to precise and improve the safety system of reference of the installation where necessary. Also, we agreed together on several pending issues.

- Factory Permanent Group meeting

The Factory Permanent Group of Experts meeting took place on November 29th 2006 and was preceded one week earlier by a visit of the installation by all the members (40 persons).

The purpose of this meeting is clearly to state on the “authorization to operate” renewal.

The expert members must be convinced by both the IRSN and CERCA that the installation and its organization are in condition to allow a safe operation. Also, it is to ensure that the tool will be improved and maintained during the next ten years.

During this meeting, the IRSN presented the conclusions of the INB 63 safety evaluation as well as the commitment of the operator as discussed during the preparatory meeting. There were some discussions between the members of the Permanent Group, the IRSN and AREVA/CERCA about pending issues. CERCA proposed an improvement plan with regard to the recommendations of the Permanent Group. This improvement plan is in progress now ad is very carefully followed by the ASN.

Finally:

« A l’issue de l’examen des documents que vous avez transmis à l’ASN et ses appuis techniques, …, je n’émets aucune objection à la poursuite de l’exploitation mentionnée en objet. »

The authorization to operate is delivered to CERCA.

- Factory Permanent Group pursue

The project does not end. It is continuing!

Our authorization to proceed is bound with our wish to make progress.

For this, the CERCA project team has been maintained in order to perform all the improvements required by the conclusions of the FPG. Whole of the actions, recommendations and commitments have been assessed and scheduled with milestones to return to the ASN.

The top management of AREVA / CERCA is very committed.

Studies and works are on-going on line with the schedule. The ASN is in charge of checking the progress of the project through regular inspections on the basis of the IRSN ratification of the CERCA files and works.

3 CONCLUSION

Getting the ASN authorization to proceed was a major issue for CERCA.

CERCA is authorized to operate till end of 2016. We were able to fit with the very high requirements level of the ASN, provided some improvements and investments.

The key factors of success of this project were mutual comprehension, confidence, full transparency and commitment between both parties.

The continuity of CERCA production is a reality in France but, why not anywhere else?

European Nuclear Society

Rue Belliard 65
1040 Brussels
Belgium
Telephone +32 2 505 30 54
Fax + 32 2 502 39 02

topsafe2008@euronuclear.org

www.euronuclear.org